Abstract Volume
6th Swiss Geoscience Meeting

Lugano, 21st – 23rd November 2008

Apply! Geosciences
6th Swiss Geoscience Meeting 2008 - Lugano

sc | nat
Geosciences
Platform of the Swiss Academy of Sciences

SUPSI
University of Applied Sciences
of Southern Switzerland
Institute of Earth Sciences

9. Natural Hazards and Risks

Giovanni Crosta, Michel Jaboyedoff

Institut de géomatique et d'analyse du risque, Université de Lausanne
Dipartimento Scienze Geologiche e Geotechnologiche, Università di Milano-Bicocca

9.1

Paleoseismological studies on Yedisu seismic gap, eastern part of North Anatolian Fault, Turkey

H. Serdar Akyüz*, Taylan Sançar**, Cengiz Zabcı*, Pınar Gutsuz**, Volkan Karabacak***, Erhan Altunel***, Ziyadin Çakır*, Çağlar Yalçıner***

*Istanbul Technical University, Faculty of Mines, Department of Geology, 34469, Maslak, Istanbul (akyuz@itu.edu.tr)
** Istanbul Technical University, Eurasia Institute of Earth Sciences, 34469, Maslak, Istanbul
***Eskisehir Osmangazi University, Engineering Faculty, Department of Geology, 26480, Eskisehir

North Anatolian Fault (NAF) is one of the most active major faults in Europe. It has a general E-W trend with about 1500 km length throughout northern Turkey and 22 ± 3 mm / year slip rate. During 20th century it is almost totally broken except two important seismic gaps; Marmara Seismic Segment in the west and Yedisu Seismic Segment in the east (Figure 1). This paper presents paleoseimological studies on Yedisu Seismic Segment (YSS).

YSS locates on eastern part of North Anatolian Fault between Erzincan city and Yedisu town of Bingöl city (Figure 2). Western part of the YSS was broken in 1992 with a Ms=6.8 earthquake while eastern part was broken in 1949 with Ms=6.7 earthquake (Figure 1). A 80 km-long fault is remained unbroken between eastern part of Erzincan Basin and Yedisu town. According to Ambraseys & Finkel (1995) this part of the fault was broken lastly in 1784, i.e. 224 years ago. The aim of this study which is supported by TUBITAK (The Scientific & Technological Research Council of Turkey, Project no: 106Y174) is to reveal seismic risk of YSS with paleoseismological data.

The fault geometry, segmentation and offset structures were analysed firstly on aerial photographs and topographical maps, then observed and drown in the field on a 1/25000 topographical map. Three trench sites were also defined in convenient places. First site was chosen in the western part of the YSS, Sarikaya site (Figure 2). Trench was opened perpendicular to the fault trace and trench wall was logged. Fine grained slope deposits and fault branches indicate two earthquake evidences. Second and third trench sites are close to eastern end of YSS (Figure 2). Karapolat Trench was opened perpendicular to fault on distal part of a large recent fan deposits. Trench stratigraphy evidenced two past earthquakes as well. The last trench, named as Tokmanik, was digged deeper due to convenient underground water level. At least 5 past earthquake events were determined on the trench walls. Charcoal samples collected in critical level in all trenches were sent to Arizona University Radiocarbon Laboratory for dating. Dating results together with historical records will give us earthquake recurrence period of Yedisu Seismic Segment. If the date of past earthquakes have periodical behaviour, this will help to predict the date of future earthquake on Yedisu Fault.

REFERENCES

Ambraseys, N.N. & Finkel, C.F. 1995: The Seismicity of Turkey and adjacent areas: a historical review, 1500-1800. Eren, Istanbul, p 240.

Barka, A., Akyüz, H.S., & 18 others, 2002: The surface rupture and slip distribution of the August 17, 1999 zmit earthquake, M=7.4, North Anatolian Fault. Bull. Seism. Soc. Amer. 92, 43-60.

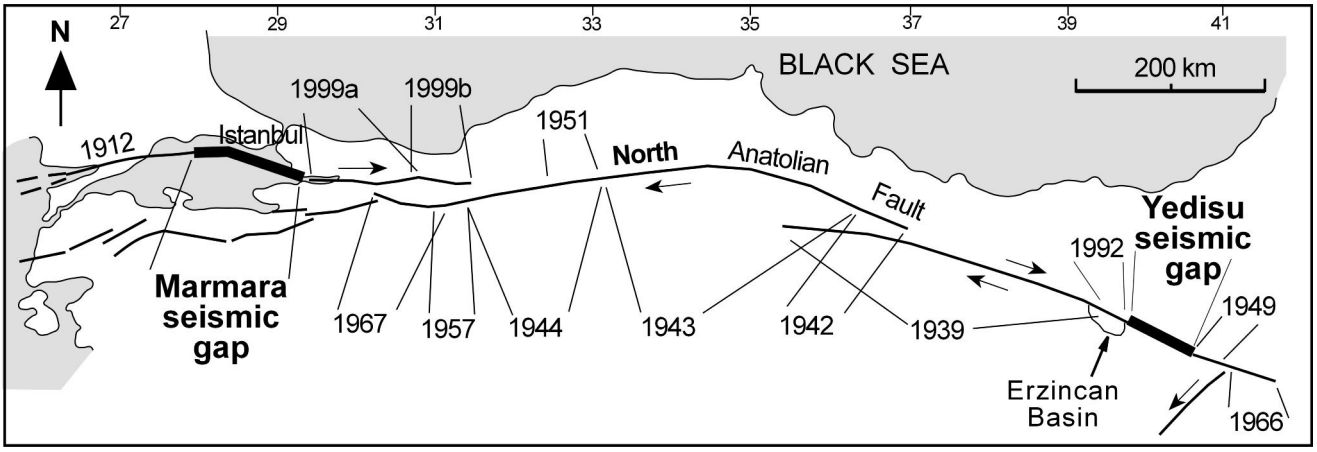

Figure 1. 20th century destructive earthquakes (Barka et al. 2002) and seismic gaps on North Anatolian Fault.

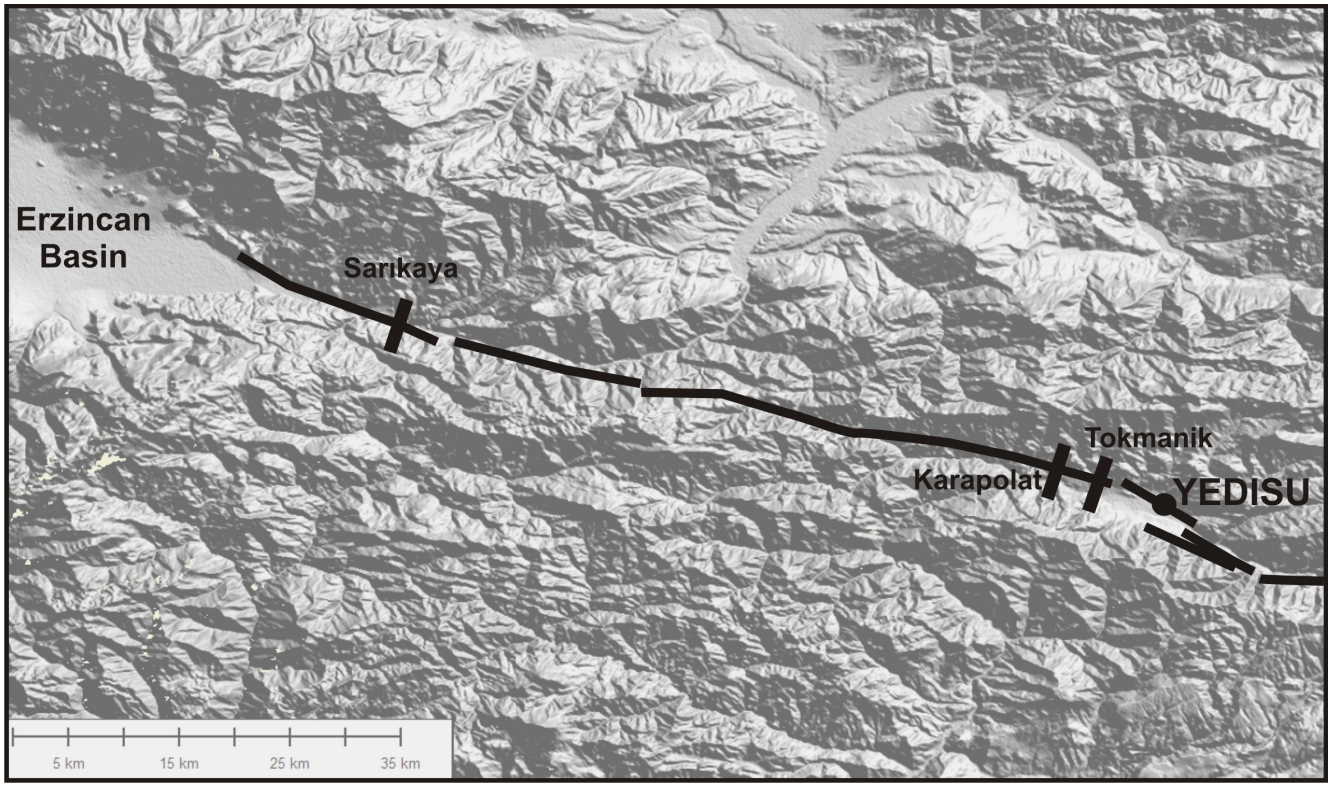

Figure 2. The geometry of Yedisu Seismic Segment and location of trench sites.

9.2

Biomarkers as effective and beneficial tools in petroleum caused natural hazards

Alizadeh Bahram*, Bagheri Soheila* & Hoseini Seyed Hossein *

*Department of Geology, Faculty of Science, S. Chamran University, Ahvaz, Iran. (alizadeh@scu.ac.ir)

In the Zagros oil rich basin comprising more than 40 huge and ten giant oilfields, unavoidebla natural hazards sometimes even force people to evacuate their homes. The aim of this study was to determine the genetic origin of oil seepages occurring in Masjid-e-Soleiman (MIS) oilfield and in Dalaki river near Nargesi oilfield. In order to inject gas in the Nargesi Oilfield (South Dezful Embayment), and at the same time prevent natural disaster it is necessary to establish the origin of oil seeps polluted with H_2S in Dalaki area.

Numerous oil seep polluted with H_2S have been found in Masjid-e-Soleiman oilfield (first oilfield in the Middle East, North

Dezful Embayment), which polluted some areas, forcing local people to leave their houses.

Asmari oil samples from Masjid-e-Soleiman oilfield correlated with oil seeps from Seeberenj and Dare-Khersan and Asmari/ Jahrum reservoir oil from Naregsi oilfield correlated with Dalaki's oil seepages by Gas Chromatography and Gas Chromatography-Mass Spectrometry.

Dalaki's oil seeps exhibit evidences of biodegradation and mix kerogens, this explains the low saturate fraction (29-38 %), the aromatic-asphaltic nature of the oil seeps and an important depletion in the homohopane series. The oil seeps are characterized by high predominance C_{29} to C_{30} hopane ratios (1.25-1.8), low ratios of C_{34} over C_{35} (1.42-1.62), and the low diasterane abundance (C_{27}-C_{29} Dia/Reg Steranes: 0.33-0.44). These characteristics suggest that the oil seeps originate from carbonate marine source rocks (Sañchez, C. & Permanyer, A., 2006). On the other hand the reservoir oil samples of Nargesi oilfield are characterized by high contents of saturates, Pr/Ph ratios below 2, the dominance of C_{30} hopanes over the C_{29} hopane (C_{29}/ C_{30}<1), low ratios of C_{34}/C_{35} (1.02- 1.4) homohopanes and diasteranes are more abundant. These properties suggest that the oils were generated mainly from marine shale facies. The C_{29}/C_{30} hopane and Dia/Reg sterane ratios and a relatively high abundance of oleanane in the oil seepages gives the best evidence of different source rocks for oil and oil seep samples. This is also supported with thermal maturity parameters such αα 20/(20S+20R) sterane and T_s/T_m ratios.

The discrepancy in the biomarker indicators gives the assurance of diverse origin of oils from reservoir and from Seepages (Fig. 1a). Finally the constant seepage discharge even after gas injection into the reservoir proved the oil correlation to be very reliable and trustworthy.

In MIS oilfield, geochemical parameters, such as high ratio of C_{27} over C_{29} sterane (1.01-1.2), the low ratio of C_{29} to C_{30} hopanes (0.63-0.71), as well as the star diagram of tricyclic terpane showed the best similarity between oil and oil seeps. For the Asmari oil and oil seepages, high ratios of steranes to hopanes are very typical (0.60 for oil and 0.48-0.63 for oil seeps) and low ratio of C_{34} over C_{35} homohopanes (0.84-1.15) that are characteristics for algae organic matter deposited within anoxic environment (Alimi et al., 2007). This is also supported by low amounts of C_{30} moretane relative to C_{30} hopane (C_{30}βα/C_{30}αβ: 0.09–0.11), indicative of strong marine input to the source rock. Both oil and oil seeps present low C_{26} over C_{25} (0.66-0.95) and C_{24}/C_{23} (0.45-0.68) tricyclic terpane ratios (less than 1), low abundance of C_{29}/C_{30} hopane (0.63-0.71) and the occurrence of diasteranes, suggest carbonate-marl source facies for oil and oil seeps.The ratios of 20S/(20S+20R) for ααα C_{29} steranes (0.48-0.51) and ββ/ (αα+ββ) for 5α-C_{29} steranes(0.5-0.54) have been evaluated together with the ratios of 22S/ (22S+22R) for C_{32} homohopanes (0.52-0.54). Based on these ratios, all samples are well within the oil window (Rogers et al., 1999). Age-specific biological marker including, Extended Tricyclic Ratio (0.5-0.52), C_{28}/C_{29} (0.79-0.89) sterane ratios, and Oleanane Index (<0.2) show that oil seeps have similar source age as Upper Jurassic-Cretaceous.

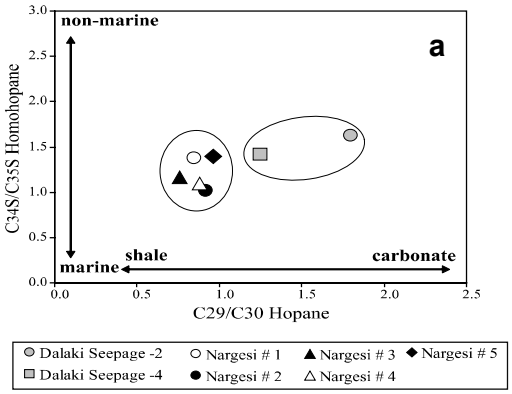

Figure1. Cross plot of C_{29}/C_{30} hopane and C_{34}/C_{35} homohopane, a, clearly indicating two different organic facies.The triangle diagram of diasterane distribution in MIS oilfield, b, demonstrating similar depositional environment for both reservoir oils and oil sepages.

The geochemical parameters showed that the oils and oil seeps were formed in similar depositional environment and have identical thermal maturity level (early oil window). In triangle diagram, (Fig. 1b), the C_{27}-C_{28}-C_{29} diasterane distribution for Asmari oil and oil seeps are located in the same vicinity indicating the source of initial organic matter being one and the same. Finally it can be concluded that the source of pollution in the area is Asmari reservoir oil and due to its pressure drop, the previously condensed H_2S poisonous gas is now free to escape through cap rock fractures, forcing people to evacuate their houses. All these well demonstrate the proficiency of geochemical parameters in predicting and managing natural hazards.

REFERENCES

Alimi, H., Alizadeh, B., Jarvie, D.M., Adabi, M.H., Tezheh, F., Jarvei, B. (2007). Geochemical Evaluation of Crude Oils from Asmari and Bangestan Reservoirs in Marun Oilfield, SW IRAN. 23rd International meeting on Organic Geochemistry, IMOG, Torquay, United Kingdom Sep. 2007.

Sa´nchez, C., Permanyer, A., 2006. Origin and alteration of oils and oil seeps from the Sinu´-San Jacinto Basin, Colombia. Organic Geochemistry, v. 37, p.1831-1845.

Rogers, K. M., Collen, J.D., Johnston, J.H., Elgar, N.E., 1999. A Geochemical appraisal of oil seeps from the East Coast Basin, New Zealand, Organic Geochemistry, v. 30 p. 593-605.

9.3

Sar Interferometric Point Target analysis and interpretation of aerial photographs for landslides investigations in southern switzerland

Ambrosi Christian*, Strozzi Tazio**

* *SUPSI, Istituto Scienze della Terra CP 72, CH 6952 Canobbio (christian.ambrosi@supsi.ch)*
** *GAMMA Remote Sensing, Worbstrasse 225, CH 3073 Gümligen (strozzi@gamma-rs.ch)*

Information on landslide displacement from SAR Interferometric Point Target Analysis (IPTA) and sketch maps from aerial photography interpretation are combined for the study of landslides in Ticino, Southern Switzerland. For current ITPA investigations, ENVISAT and RADARSAT SAR acquisitions over the Swiss territory are used. Numerous unstable phenomena are considered in this mountainous region, with an elevation range from approximately 200 m a.s.l. to more than 3000 m a.s.l. The results achieved with IPTA are attractive to complement aerial photographs interpretation for the evaluation of the state of activity of landslides over villages and in sparsely vegetated areas with numerous exposed rocks. On the other hand, over vegetated areas (forests and meadows) IPTA failed to retrieve displacement information. Because displacement from InSAR is recorded along the satellite line-of-sight direction, IPTA cannot be directly use for the determination of the intensity of landslides in hazard mapping. In general, the actual displacement rate is larger than that recorded with InSAR. Over alpine areas characterized by sparse vegetation, where snow cover limits the availability of a large number of SAR acquisitions, conventional InSAR was successfully applied to estimate the motion of rockglaciers and other periglacial phenomena. For vegetated areas and relatively rapid landslides L-band InSAR (JERS-1 SAR and ALOS PALSAR) has been found to be an efficient solution.

9.4

Interdisciplinary approaches to recognition, analysis and modelling in sackung system and large landslides in southern Swiss Alps

Ambrosi Christian*, Pera Sebastian*

* *SUPSI, Istituto Scienze della Terra CP 72, CH 6952 Canobbio (christian.ambrosi@supsi.ch)*

A very large Deep-Seated Gravitational Slope Deformations and large landslides, affecting the slopes of Swiss Southern Alps, have been recognised and mapped. Several active rotational and translational deep seated landslides occur in the lower part of the slopes, often in association with rockslides at different scale. These phenomena show a different stage of evolution along the flanks of the ridges.
Some of these landslides (Pontirone, Osco, Faido) has been recognised through different techniques. In particular, it has been characterised by aerial photo interpretation, field surveys, tracer tests and analysis of detailed airborne Lidar DEM.
Rock masses, including poly-deformed orthogneisses, paragneisses and dolostones, are affected by systems of impressive gravitational morpho-structures including ENE trending open trenches, scarps and counterscarps forming graben-like structures.
Geodetic measurements (optical targets and GPS points) and satellite radar interferometry (DinSAR) data demonstrate the activity of the gravitational features affecting both the upper and lower part of the slopes.
The analysis of geological, geomorphological, hydrogeological, in situ stress, geodetic and uplift data, have been used to demonstrate the possible relationships among geological, structural, topographic and gravitational features. Numerical 2D modelling have been used to evaluate failure in presence of elastic, elasto-plastic materials and groundwater flow. This allow to verify “model” sensitivity to some factors as slope geometry, structural features, groundwater conditions and to determinate the triggers factors of these instabilities.
On this basis we discuss the possibility that the geological, tectonic and hydrogeological framework can play an active/passive role in the onset and development of the sackung system and related landslides.

9.5
A GIS-tool for risk assessment due to natural hazards in mountain regions

Baruffini Mirko*, Baruffini Moreno* & Thüring Manfred*

*Istituto Scienze della Terra IST-SUPSI, C.P. 72, CH-6952 Canobbio (ist@supsi.ch)

During the last decades land-use increased significantly in the Swiss (and European) mountain regions. Due to the scarceness of areas suitable for development, anthropic activities were extended into areas prone to natural hazards such as avalanches, debris flows and rockfalls (Smith 2001). Consequently, an increase in losses due to hazards can be observed. To mitigate these associated losses, both traditional protective measures and land-use planning policies are to be developed and implemented to optimize future investments. Efficient protection alternatives can be obtained considering the concept of integral risk management.

Risk analysis, as the central part of risk management, has become gradually a generally accepted approach for the assessment of current and future scenarios (Loat & Zimmermann 2004). The procedure aims at risk reduction which can be reached by conventional mitigation on one hand and the implementation of land-use planning on the other hand: a combination of active and passive mitigation measures is applied to prevent damage to buildings, people and infrastructures.

Considering different hazard processes and their impact on the built environment, multiple solutions for the protection of new buildings and infrastructures and the upgrade of existing inventory exist. Consequently, the concept of local protection should be embedded within the framework of integral risk management strategies. Planned early, expenditures for the implementation of local structural measures are comparatively low related to the total cost of the planned construction. Recent studies suggested a considerable decrease in vulnerability, if local structural protection is implemented (Holub & Fuchs 2008).

As part of the Swiss National Science Foundation Project 54 “Evaluation of the optimal resilience for vulnerable infrastructure networks - An interdisciplinary pilot study on the transalpine transportation corridors” we study the vulnerability of infrastructures due to natural hazards.

The Swiss system for risk analysis of gravitational natural hazards (BUWAL 1999) offers a complete framework for the analysis and assessment of risks due to natural hazards, ranging from hazard assessment for gravitational natural hazards, such as landslides, collapse, rockfall, flooding, debris flows and avalanches, to vulnerability assessment and risk analysis, and the integration into land use planning at the cantonal and municipality level. The scheme is limited to the direct consequences of natural hazards.

We conduct a research referred to the concept of the evaluation of the resilience within the framework of integral risk management with the aim to develop a system which integrates the procedures for a complete risk analysis in a Geographic Information System (GIS) toolbox, in order to be applied to our testbed, the Alps-crossing corridor of St. Gotthard.

A simulation environment, RiskBox, is developed within the open-source GIS environment GRASS (Geographic Resources Analysis Support System) and a database (PostgreSQL) in order to manage a infrastructure data catalog. The targeted simulation environment includes the elements that identify the consecutive steps of risk analysis: hazard – vulnerability – risk.

Module hazard integrates applications to simulate natural hazard processes in order to assess their degree of hazard. Module vulnerability integrates vulnerable objects and attributes them with the necessary meta-data. Module risk integrates the necessary analysis approaches in order to conduct the risk analysis based on the former two modules.

The final goal of RiskBox is a versatile tool for risk analysis which can be applied to other situations. There are specific needs for an improvement of the level of information for affected people, legal regulations and risk transfer mechanisms (ARMONIA Project 2007). These needs would not only result in an increased risk awareness of people concerned, but also in an enhanced enforceability of necessary legal regulations, such as land-use planning rules and building codes. So, the individual responsibility could be strengthened and the society will be enabled to an alternatively use of the resources in a more cost-efficient way.

The initial results of the experimental case study shows how useful a GIS-based system can be for effective and efficient disaster response management.
We present the concept and current state of development of RiskBox and its application to the testbed, the Alps-crossing corridor of St. Gotthard.

REFERENCES
ARMONIA Project 2007: Land use plans in Risky areas fro Unwise to Wise Practices – Materials 2nd conference. Politecnico di Milano.
BUWAL 1999: Risikoanalyse bei gravitativen Naturgefahren - Methode, Fallbeispiele und Daten (Risk analyses for gravitational natural hazards). Bundesamt für Umwelt, Wald und Landschaft (BUWAL). Umwelt-Materialen Nr. 107, 1-244.
Holub, M. & Fuchs S. 2008: Benefits of local structural protection to mitigate torrent-related hazards. In: Brebbia, C.A. & Beritatos, E. (eds) 2008: Risk Analysis VI: Simulation and Hazard Mitigation. Institute of Technology, UK and University of Thessaly, Greece, 401-411.
Loat, R. & Zimmermann, M. 2004 : La gestion des risques en Suisse (Risk Management in Switzerland). In: Veyret, Y., Garry, G., Meschinet de Richemont, N. & Armand Colin (eds) 2002: Colloque Arche de la Défense 22–24 octobre 2002, dans Risques naturels et aménagement en Europe, 108-120.
Smith, K. 2001: Environmental hazards. Assessing the risk and reducing disaster. Third edition. London

9.6

Multidisciplinary investigations and back-analysis of a periglacial rock fall event: Tschierva rock fall

Fischer Luzia *, Amann Florian**, & Huggel Christian*

* *Glaciology, Geomorphodynamics & Geochronology, Department of Geography, University of Zurich, Switzerland (luzia.fischer@geo.uzh.ch)*
** *Group of Engineering Geology, Department of Earth Science, ETH Zurich, Switzerland*

Slope stability of steep rock walls in glacierised and permafrost-affected high-mountain regions is controlled by many different factors such as geological and geomechanical characteristics, topography, hydrology and also glaciation and permafrost occurrence. Changes in one or more of these factors may reduce the slope stability and eventually lead to a rock fall event. The atmospheric warming during the 20th century has caused pronounced effects in the glacial and periglacial belts of high mountain areas. The changes are made strikingly evident by, for example, the retreat of Alpine glaciers and less immediately visible but also very significant are changes in mountain permafrost distribution and temperature. Therefore, cryospheric factors are most prone to ongoing climate changes. In this study the influence of different factors and mechanisms determining slope stability is investigated, based on a case study of the Tschierva rock fall event.

The Tschierva rock fall occurred on October 19, 1988 from the western flank of Piz Morteratsch (3751 m asl, Engadin, Switzerland) on Tschierva glacier with an estimated volume of approximately 0.3x10^6 m^3. The rock mass detached at about 3200 m a.s.l. and fell on the Tschierva glacier probably incorporating additional rock-debris from the slope below the detachment zone and stopped on the glacier at an elevation of about 2700 m a.s.l.

The primary objective of the presented study is the back-analysis of the Tschierva rock fall and the investigation of possible geological, geomechanical and climate-related glaciological disposition factors. Therefore, the detachment zone is investigated in a multidisciplinary approach based on in-situ geological field work, associated geotechnical investigations, morphometric analyses, permafrost modelling, glaciation history and subsequent numerical stability modelling with UDEC (Universal Distinct Element Code by Itasca). Based on these analyses, the influence and sensitivity of the different factors and processes on the slope failures is assessed.

Numerical slope stability modeling was performed to examine different scenarios of possible failure mechanisms. Modelling of the unloading of the pleistocene glacial overburden showed that subsequent redistribution of stress and strain fields in the flank have a strongly controlling influence on the geometry of the detachment zone by the opening of unloading joints. A sensitivity analysis of geotechnical parameters additionally showed that the cohesion of the discontinuities was a fundamental parameter. Coupled hydro-mechanical modeling demonstrated that slope stability was very sensitive to changes in water pressure. The existing fault zone crossing the rock slope induced an elevated water inflow due to the higher permeability and might therefore be, together with the long-lasting effects of ice unloading, a main factor for the slope instability.

In conclusion, our analysis could identify some essential factors of slope stability in relation with the geological setting, glacier retreat and permafrost degradation. However, it has also shown that the understanding of the physical processes and the adequate integration in numerical slope stability models needs more research, in particular in view of the hazards that are to be faced.

9.7

Applying altimetry and in-situ data to compute point-wise MSL for inland waters, case study: Caspian Sea

Forootan Ehsan*, Sharifi Mohammad Ali*, Nikkhoo Mehdi**, & Dodge Somayeh***

* *Surveying and Geomatics Engineering Department, College of Engineering, University of Tehran. Northern Amirabad St, Tehran, Iran, Tel:00982161114251, Fax:00982188008837 ({eforootan | sharifi }@ut.ac.ir)*
** *Surveying and Geomatics Engineering Department, KNT University of Technology, Iran. mehdi_nikkhoo@yahoo.com*
***University of Zurich, Winterthurerstr. 190, CH-8057 Zurich*

The Caspian Sea is the largest enclosed body of water on the Earth by area, variously classed as the world's largest lake or a full-fledged sea. The sea is fed by numerous rivers including the Volga, Ural, Terek, and Kura rivers. In the last 25 years, the total surface area has varied from 360000 to 400000 km^2 due to high water level variations. These variations have shown oscillations between -26 and -29 meters (with respect to the zero ocean level) during the last hundreds years.
The largest uncertainty for the Caspian Sea is concerning with the average water level, which by itself is not subject to a statistical distribution, but rather more to a trend. Hence, we applied two major datasets to compute the water fluctuations: 1) in- situ measurements; in this case provided by the Iranian Caspian environmental study center. 2) derived water levels from satellite altimetry mission; we used T/P altimeter data, which are performed, at the Jet Propulsion Laboratory, California and cover repeated T/P mission cycles 11 to 400, spanning more than 10 years. The results of these observations are considered as a set of virtual tide gauges, with a sample rate of every 9.915625 days. Beside that, we applied in-situ observations to reveal the trend and evaluate the altimetry results.
Analysis of T/P observations show that there is a phase differences between various locations in the Sea. In fact, 80% of the input side of the water balance influx comes from the Volga River. It seems that the cause of these differences is related to the distance between locations to the River of Volga. Change in discharge of Volga does not expand all over the sea immediately but the locations that are nearer to the outfall of the river are influenced sooner than the other locations. Therefore, it is necessary to investigate the variations of each point in the Caspian Sea separately in order to discover the environmental variables using time series analysis and then computing the point-wise MSL.
In short the results of our analysis proved that between January 1993 and March 1995 the Caspian mean sea level rose at an average rate of 15 mm/month then followed by a fall at a rate of -5.5 mm/month until January 2003. Beside that, a point-wise MSL is computed for the Caspian Sea during 1993 to 2002. The results will be discussed in more detail in the full paper.

REFERENCES

Avakian, A. B. and V. M. Shirokov. 1994. Rational Use and Protection of Water Resources. Ekaterinburg: Publ. House "Victor" (in Russian).

Benada, J. R., 1997, TOPEX/POSEIDON User's Handbook , Generation B (MGDR-B) Version 2.0, D-11007, Jet Propulsion Laboratory, California Institute of Technology under contract with the National Aeronautics and Space Administration.

Birkett, C.M., 1995a: The contribution of TOPEX/POSEIDON to the global monitoring of climatically sensitive lakes, JGR-Oceans, Vol.100, C12, pp.25, 179-25, 204

Caspian TDA, report volume 2, 2002., Transboundary diagnostic analysis for the Caspian sea. The Caspian sea environment programme., Baku, Azerbaijan. www.caspianenvironment.org

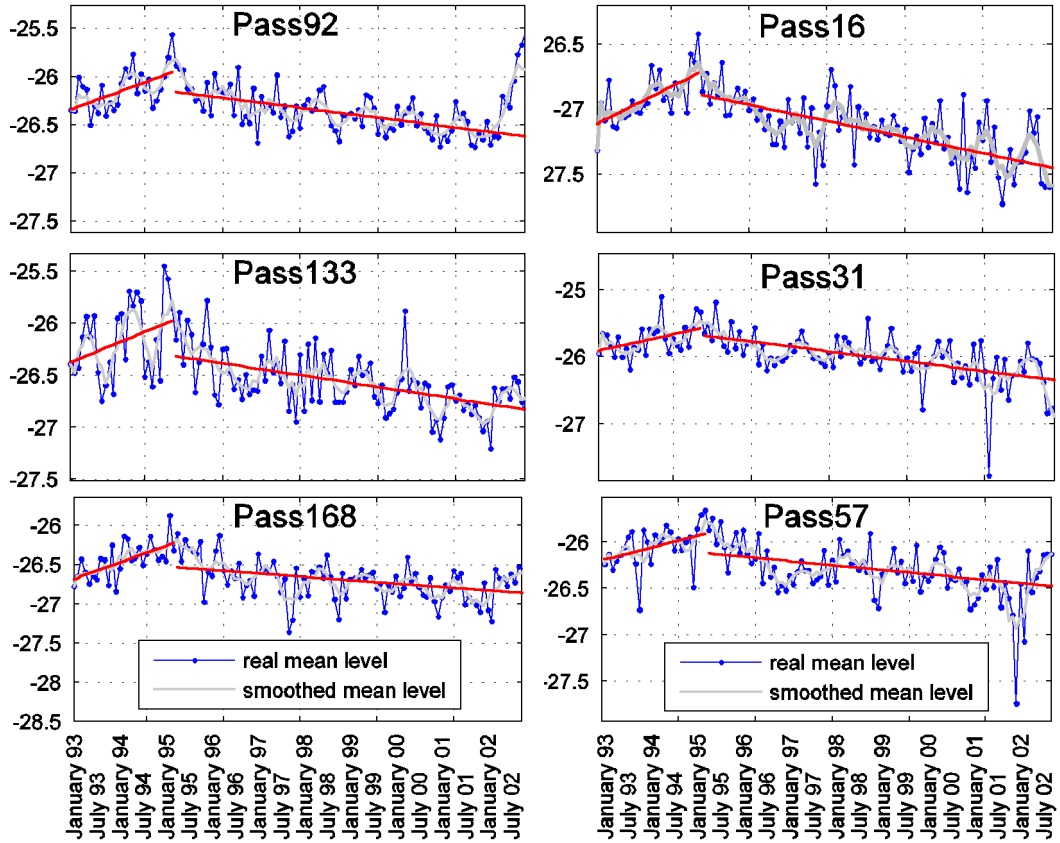

Figure 1. Mean level variations of SSH along 6 passes in Caspian Sea.

9.8

The Deep Seated Gravitational Slope Deformation of Landarenca (Graubünden, Switzerland): A Geological-Geotechnical Analysis

Fossati David*, Kos Andrew*

*Group of Engineering Geology, Geological Institute, Wolfgang-Pauli-Str. 15, 8093 Zürich (fossatid@student.ethz.ch)

A complex deep seated gravitational slope deformation (DSGSD) located in the south western part of the Calanca valley (Graubünden, Switzerland), in the area of Landarenca will be described using an multi-disciplinary approach, where field surveys, remote sensing and geodetic measurements are applied to the site for the first time. The DSGSD lies within isoclinally folded gneisses and mica schists of the Adula and Simano nappes. Geomorphologic features such as terraces, steep rock cliffs, tension cracks, scarps, counterscarps and combined scarp-tension crack structures characterize the area. The area of the DSGSD involves at least 1 square kilometre with an approximate volume of 185 million cubic meters. An integration of results indicate the DSGSD to be slightly active with velocities of up to 8mm per year. Movements involve discontinuous creeping, i.e. a combination of creeping and sliding and the DSGSD can be defined as a slightly active, deep seated kink band slumping, in a developed stage.

REFERENCES

Amann, F. 2006: Grosshangbewegung Cuolm da Vi (Graubünden, Schweiz) – geologisch-geotechnische Befunde und numerische Untersuchungen zur Klärung des Phänomens. Diss. Univ. Erlangen-Nürnberg.

Agliardi, F., Crosta, G. & Zanchi, A. 2001: Structural constraints on deep-seated slope deformation kinematics. Eng. Geol. 59 (1-2), 83-102.

Kieffer, D. S. 1998: Rock slumping: A compound failure mode of jointed hard rock slopes. PhD Thesis. University of California, Berkeley.

9.9

Recent experiences from Swiss projects in risk reduction in South America

Christian Huggel*, Sebastian Eugster**, Juan Manuel Ramírez***, Raphael Worni*, ****

Glaziologie, Geomorphodynamik & Geochronologie, Geographisches Institut, Universität Zürich, Winterthurerstrasse 190, 8057 Zürich (christian.huggel@geo.uzh.ch)
Swiss Agency for Development and Cooperation, Lima, Peru
Swiss Agency for Development and Cooperation, Bogotá, Colombia
Department of Environmental Sciences, ETH Zürich

Extensive parts of South America are characterized by mountain topography and seasonally intense rainfall. Accordingly many regions suffer from repeated landslides, debris flows, floods. These hazards are partly linked, and exacerbated by volcanic activity along the Andean mountain chain. Additionally, in some regions of the Andes, disasters related to glaciers have claimed thousands of victims. Such extreme events occurred in the 1970s in Peru with an ice-rock avalanche from Huascaran and in the 1980s in Colombia with lahars from Nevado del Ruiz. Since the time of these disasters important advances in disaster risk reduction have been made on the national levels. In Colombia, for instance, the failures related to the Ruiz disaster triggered the creation of a National System for Prevention and Attention of Disasters (SNPAD).
However, it continues to be important to improve the current situations to avoid any significant type of disaster. Critical improvements can be made on an institutional and community-based level, combined with the implementation of advanced technological and scientific know-how. Effective disaster risk reduction takes place on a local level but is embedded in the regional and national institutional context.
Here we report on recent experiences from projects of the Swiss Government (Swiss Agency for Development and Cooperation, SDC) in collaboration with the University of Zurich and several national institutions in Colombia and Peru. In Peru, a Peruvian – Swiss programme on adaptation to climate change (PACC) has recently been initiated and aims at identifying climate change impacts in the Andean Cuzco and Apurimac regions in Peru, and to implement a set of adaptation measures to reduce adverse effects of climate change. The PACC focuses on three major areas: (i) disaster risk reduction; (ii) water resource management; and (iii) food security. In a climate change context it is particularly important to approach risk reduction in an integrated perspective considering the related areas and combined effects.
In Colombia, activities have focused on volcanoes, glaciers and rainfall triggered landslides. The 2007 crisis and eruption of Huila Volcano has made necessary a close collaboration of science and civil authorities to avoid disasters that could have been caused by major debris flows originating from volcano-ice interaction. With respect to landslides important experiences have been gained with the implementation of an early warning system.
An effective landslide early warning system is a major challenge in practice. Difficulties are found on a technical-scientific level (e.g. application of rainfall-landslide thresholds) but also on an institutional and community-based level. The early warning system is only successful if the inter-institutional coordination works smoothly in an emergency and if it is also borne by the local population. The perception of the risk by the local people in their livelihood context exerts a significant control on the response to risk reduction efforts. Their views are often diverging from those of public authorities and experts, which has to be taken into account for more effective disaster reduction.

9.10

Theoretical basis for shadow angle variability and implications

Jaboyedoff Michel*, Pedrazzini Andrea*

* *Institute of Geomatics and Analysis of Risk, Faculté des géosciences et de l'environnement, University of Lausanne, CH-1015 Lausanne - Switzerland (michel.jaboyedoff@unil.ch)*

Since Heim (1932) the shadow angle or Farböschung has been widely studied to estimate runout distance of landslides (Corominas, 1996). The distance used to determine the shadow angle is based either on the maximum of runout distance or on a threshold distance (Evans and Hungr, 1993; Toppe, 1987). This discrepancy for empirical approach has to be explained.

In the present paper we inspected the uncertainty on the parameters of the simple model of the energy line. The uncertainty that is relevant comes essentially from the friction parameter. As a consequence the friction coefficient can be assumed as a random variable along the landslide path. As it is a sum of random variables it must follow a normal distribution owing to the central limit theorem.

This hypothesis can be verified on several landslide data sets such as rock falls, shallow landslides, snow avalanches, etc. In any case, this permits to unify all the different approaches taking into account the difference between energy line and Farböschung.

REFERENCES

Corominas J. 1996: The angle of reach as mobility index for small and large landslides. Can Geotech J 33:260–271.
Heim A. 1932: Bergsturz und Menschenleben - Fretz und Wasmuth, Zurich, 218 pp.
Evans, S., Hungr, O., 1993: The assessment of rockfall hazard at the base of talus slopes. Canadian Geotechnical Journal, 30, 620-636.
Toppe, R. 1987: Terrain models: a tool for natural hazard mapping. In: Avalanche formation, movement and effects. Edited by B. Salm &H. Gubler. International Association of Hydrological Sciences. Wallingford, UK. Publication 162, pp. 629-638.
297, 269-281.

9.11

Machine learning algorithms for spatial data. Case studies: environmental pollution, natural hazards, renewable resources

Kanevski Mikhail*, Pozdnoukhov Alexei*, Timonin Vadim*

**Institute of Geomatics and Analysis of Risk (IGAR), University of Lausanne, CH-1015 (Mikhail.Kanevski@unil.ch)*

This paper presents general problems and approaches for the spatial data analysis using machine learning algorithms. Machine learning is a very powerful approach to adaptive data analysis, modelling and visualisation. The key feature of the machine learning algorithms is that they learn from empirical data and can be used in cases when the modelled environmental phenomena are hidden, nonlinear, noisy and highly variable in space and in time. Most of the machines learning algorithms are universal and adaptive modelling tools developed to solve basic problems of learning from data: classification/pattern recognition, regression/mapping and probability density modelling.

In the present report some of the widely used machine learning algorithms, namely artificial neural networks (ANN) of different architectures and Support Vector Machines (SVM), are adapted to the problems of the analysis and modelling of geo-spatial data. Machine learning algorithms have an important advantage over traditional models of spatial statistics when problems are considered in a high dimensional geo-feature spaces, when the dimension of space exceeds 5. Such features are usually generated, for example, from digital elevation models, remote sensing images, etc. An important extension of models concerns considering of real space constrains like geomorphology, networks, and other natural structures. Recent developments in semi-supervised learning can improve modelling of environmental phenomena taking into account on geo-manifolds. An important part of the study deals with the analysis of relevant variables and models' inputs. This problem is approached by using different feature selection/feature extraction nonlinear tools.

To demonstrate the application of machine learning algorithms several interesting case studies are considered: digital soil mapping using SVM, automatic mapping of soil and water system pollution using ANN; natural hazards risk analysis (avalanches, landslides), assessments of renewable resources (wind fields) with SVM and ANN models, etc. The dimensionality of spaces considered varies from 2 to more than 30.

Figures 1, 2, 3 demonstrate some results of the studies and their outputs.

Finally, the results of environmental mapping are discussed and compared with traditional models of geostatistics.

Acknowledgements. The study was partially supported by the Swiss National Science Foundation projects GeoKernels (project No 200021-113944) and Clusterville (project No 100012-113506).

REFERENCES

Kanevski, M. (Editor), 2008. Advanced Mapping of Environmental Data. ISTE Ltd., John Wiley & Sons Inc, 313 pp.

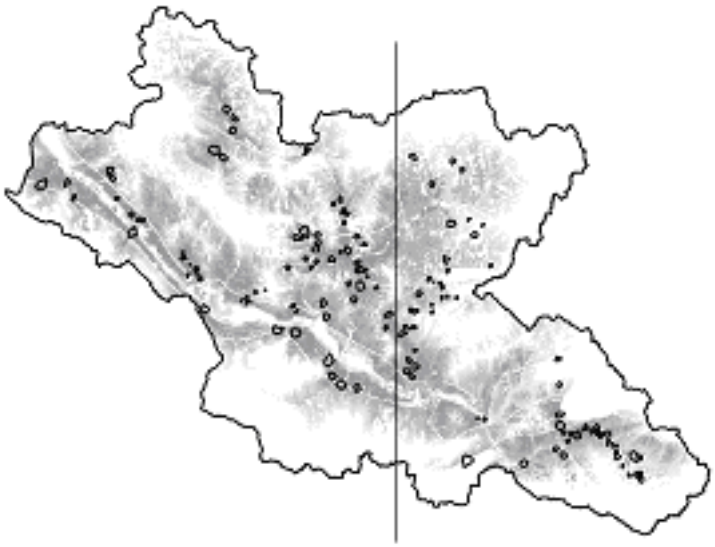

Figure 1. Map of potential areas where landslides can occur (region of the study - northwest China). Darker colours present regions with higher probability of danger. Training areas (outlined by polygons) are also presented.

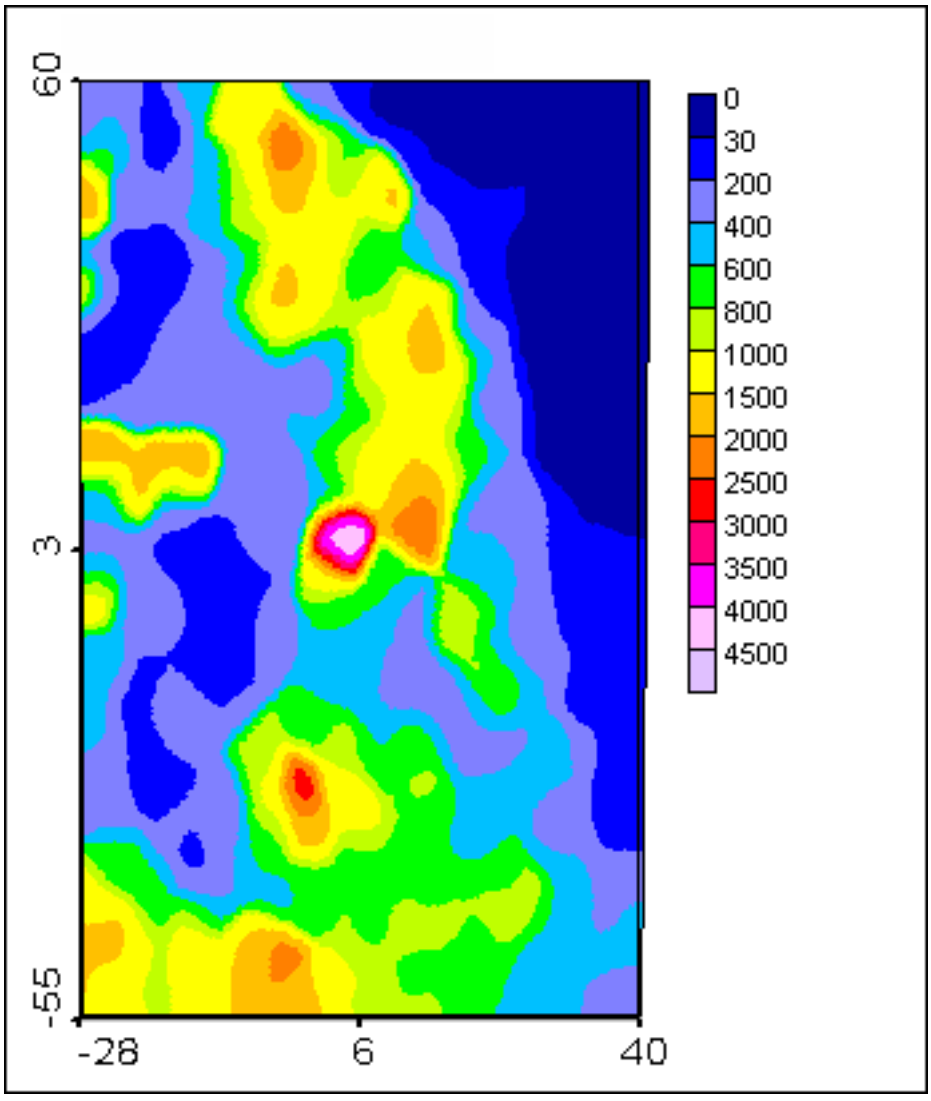

Figure 2. Map of soil pollution automatically generated by ANN.

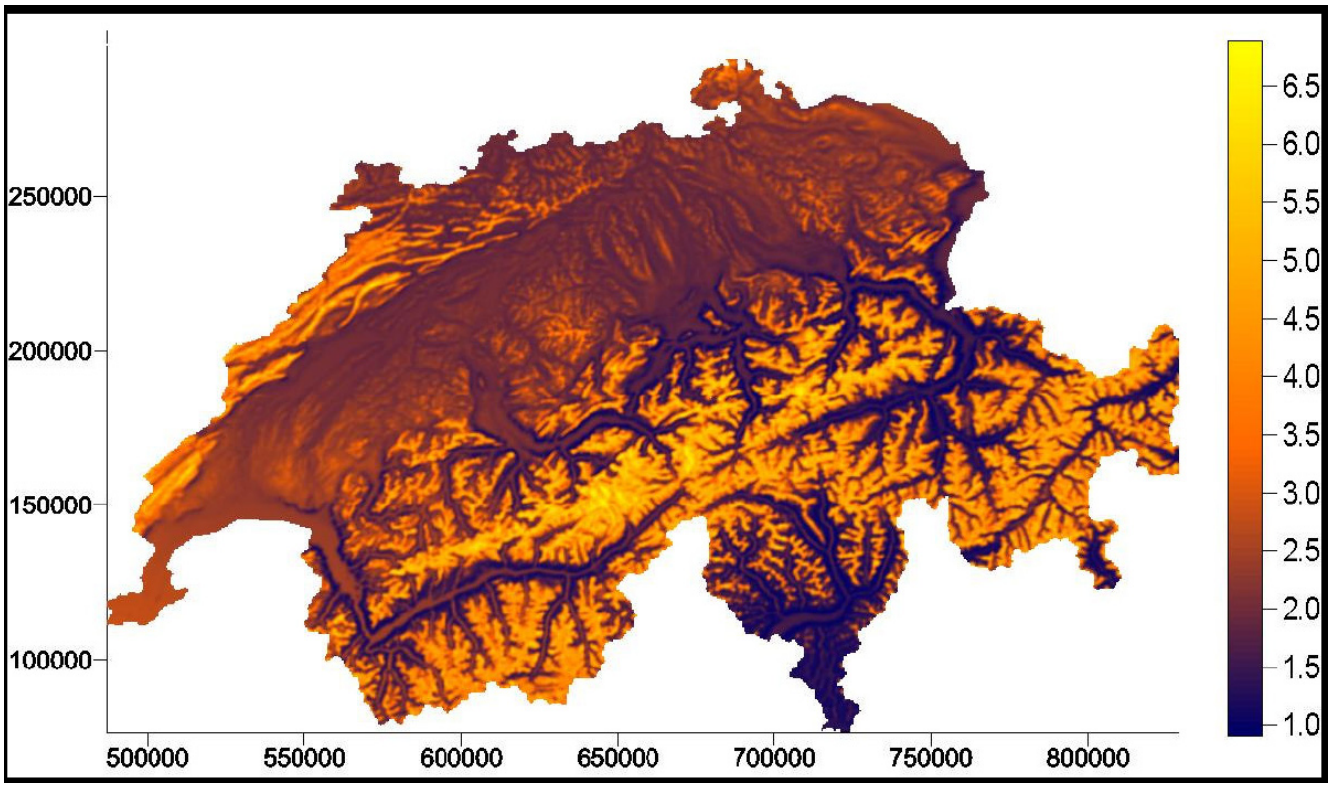

Figure 3. Map of wind fields in Switzerland.

9.12

A method for risk analysis related to lahars and floods – a case study at Nevado del Tolima volcano, Colombia

Künzler Matthias*, Huggel Christian*, Ramírez Juan Manuel**

*Department of Geography, University of Zurich, Winterthurerstrasse 190, CH-8057 Zurich (mkuenzler@access.unizh.ch, christian.huggel@geo.uzh.ch)
**Swiss Agency for Development and Cooperation, Bogotá, Colombia

The glacier-covered Nevado del Tolima located in the Colombian Cordillera Central (Figure 1) is an active volcano with potential lahar hazards similar to those on Nevado del Ruiz (Thouret et al., 1995). For effective disaster prevention a risk analysis is an important tool. We present here a methodology that allows for a relatively rapid assessment of the risk based on a first-order analysis of lahar and rainfall related flood hazards, and vulnerability. The methodology is performed for five villages in the Combeima Valley and the regional capital Ibagué (≈450,000 inhabitants).

Firstly, the models LAHARZ for lahars and HEC-RAS for floods were applied to generate hazard maps. Lahar scenarios are based on melting of 0.5, 1, 5, and 15 m of glacier ice due to volcanic activity, resulting in lahar volumes of 0.5, 1, 5, and 15 million m^3. For flood modelling, design floods with a return period of 10 and 100 years were calculated. A second step involves the analysis of different vulnerabilities. Physical vulnerability is operationalised by market values of dwelling parcels and population density, whereas social vulnerability is expressed by population age and poverty. Thirdly, hazard H and vulnerably V values are both transformed into a scale from 0 to 1 and subsequently multiplied following the risk equation $R = H * V$ (Varnes, 1984). The results are qualitatively risk values per parcel level and quantitative damage estimates. Figure 2 schematically illustrates the risk analysis concept. The left side refers to the vulnerability and the right side to the hazard, respectively. Grey parallelograms are GIS layers.

Whereas flood hazard has limited effects on population and infrastructure, the impact of lahars is more serious. An assumed lahar volume of 15 million m^3 may lead to lahar heights of 19 m and a maximum horizontal cross section of ca. 450 m. Over 20,000 people may be affected.

While uncertainties yet prevail with respect to the topographic basis and hazard mapping in general, the overall methodology has proven to be a suitable tool to provide a first overview of spatial distribution of risk, helpful for decision-makers. We should consider, however, that the weighting of the different vulnerabilities has an important control on resulting risks and should therefore be performed in coordination with the responsible authorities.

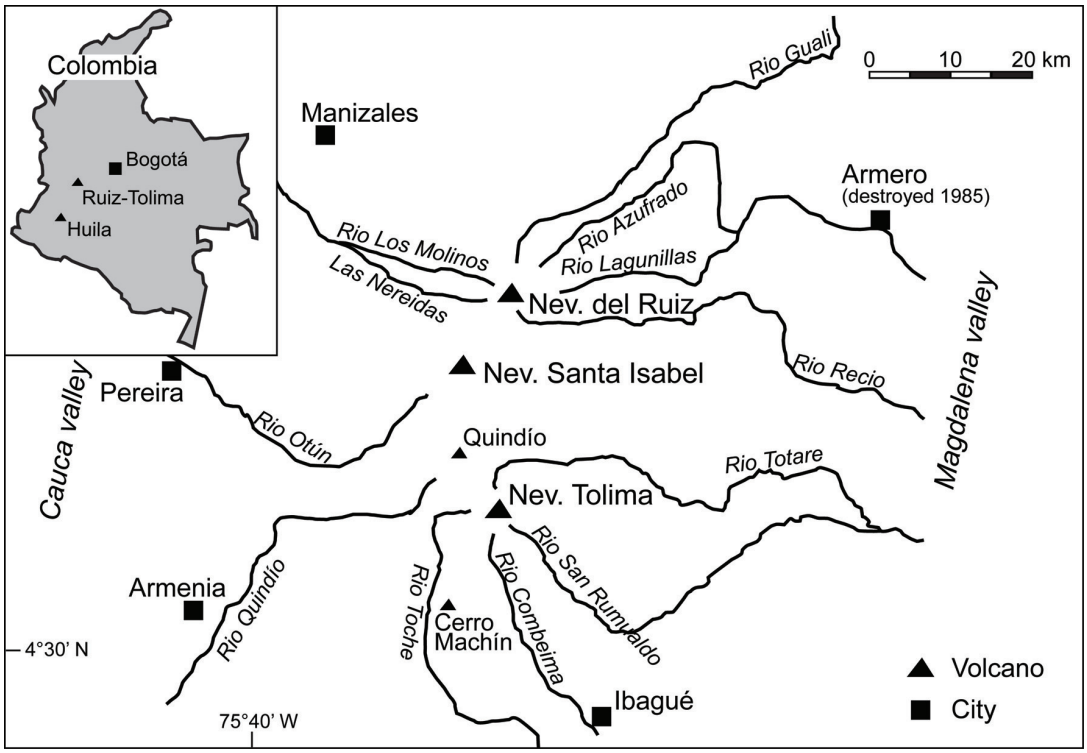

Figure 1. Cordillera Central with Nevado del Tolima and Nevado del Ruiz (from Huggel et al., 2007).

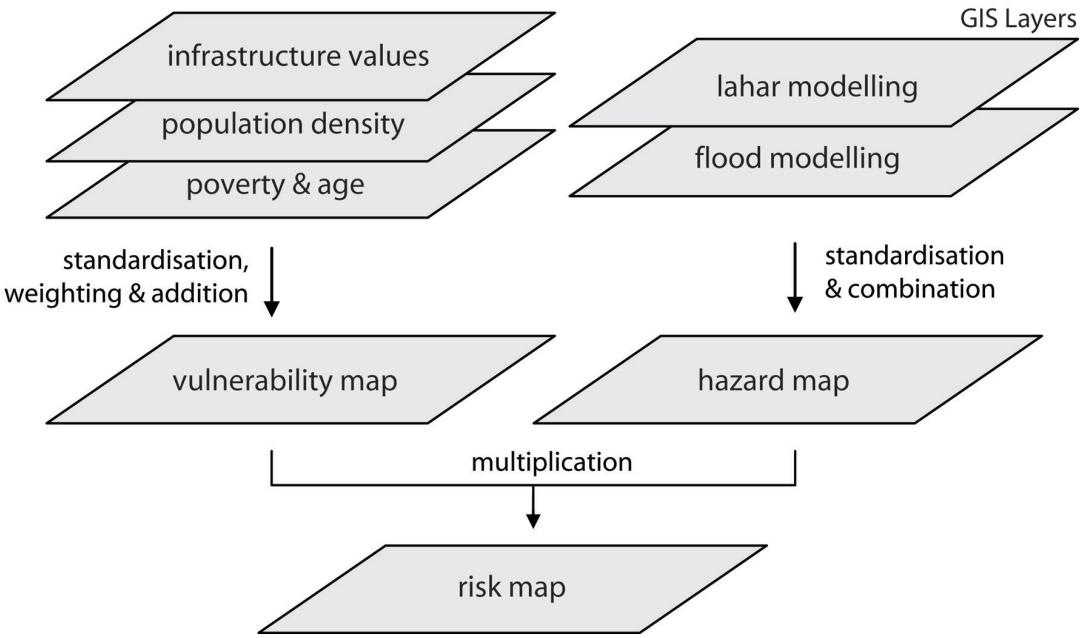

Figure 2. Flow chart of the risk analysis concept based on a *R=V*H* approach.

REFERENCES

Huggel, C., Ceballos, J.L., Pulgarín, B., Ramírez, J. & Touret, J.-C. 2007: Review and reassessment of hazards owing to volcano-glacier interactions in Colombia. Annals of Glaciology, 45, 128-136.

Thouret, J.-C., Cantagrel, J.-M., Robin, C., Murcia, A., Salinas, R. & Cepeda, H. 1995: Quaternary history and hazard-zone model at Nevado del Tolima and Cerro Machin Volcanoes, Colombia. Journal of Volcanology and Geothermal Research, 66, 397-426.

Varnes, D.J. 1984: Landslide hazard zonation: a review of principles and practice. United Nations Educational, Scientific and Cultural Organisation, Paris. 63 pp.

9.13

Geological heterogeneity in landslides: Characterization and flow modelling

Boris Matti

SUPSI, Istituto Scienze della Terra CP 72, CH 6952 Canobbio (boris.matti@supsi.ch)

Significant progress has been made these last decades in the development of hydrogeological numerical flow modelling for describing the hydrodynamic behaviour of landslides. However, these new sophisticated methods are still very seldom used in the problems of slope instability in particular because of the hydrogeological complexity which characterizes them; thin aquifers, discontinuous media, succession of saturated and unsaturated zones, low permeabilities, high hydraulic gradients, lithological heterogeneity, strong contrasts of permeabilities and heterogeneous infiltration.

Predictive models of flow in the subsurface, which are often based on homogeneous porous media types of representation, are badly adapted to natural systems that are characterized by highly heterogeneous media such as landslides. These models are good and reliable on a landslide scale (regional scale), but their quality may be affected on a local scale by strong geological heterogeneities. Geological heterogeneities of the subsurface take part in determining the hydrodynamical and geomechanical behaviour of landslides. However, their spatial distribution is partially unknown.

Thus, the principal objectives of this work are: (i) To carry out an integrated multidisciplinary characterization study on the internal structure of landslides in flysch and Quaternary environments, in order to clarify the organisation of the geological heterogeneities and to identify the hydrodynamic implications. (ii) To propose a conceptual model representing the geological architecture and the hydrogeological functioning. (iii) To examine the effects of heterogeneity and anisotropy on flow systems. (iv) To better understand the influence of geological heterogeneities on the mechanical behaviour of large landslides by performing numerical sensitivity analyses, by means of different heterogeneity scenarios on the field parameters. (v) Finally, to test the incidences on slope stabilization techniques; evaluation of the efficiency of a drainage gallery work. The main test site of *la Frasse landslide* (VD, Switzerland) was chosen, and completed with additional landslide cases.

The main results are the following:

In most of the case studies, the landslide mass is composed of an old prehistoric stabilized mass, pinched between the active sliding mass and the bedrock, and playing an important hydrologic role. The stabilized mass and the bedrock form the substratum of the landslide.

Landslides occurring in these types of media are defined by an organized heterogeneous environment with “fracture” flows and discontinuity porosity. The overall hydraulic conductivity is low, and locally high permeable zones exist. Regional groundwater circulations are limited and form local interconnected aquicludes organised in thin aquifers, and presenting saturated and unsaturated zones.
The hydrogeological analyses showed that the system presents a bimodal permeability; (i) Low hydraulic conductivities characterizing the global matrix and defining the capacitive fraction, and (ii) high permeable features, with high hydraulic conductivities defining the conductive fraction, and favouring strong channelling effects. Besides, the observation shows that the aquifer system is generally very reactive with important magnitudes. Often, there is a straight correlation between water level variation and climatic conditions (rainy events).
Landslides are characterized by two important inflows namely effective infiltration from the surface and lateral inflows from the neighbouring units. Water transfer between the stabilized mass and the active mass may be important and thus have to be considered. The existence of water transfer between the bedrock and the landslide mass (stabilized and active) is not well established. The bedrock and the landslide mass present a hydrological behavioural independence.

Theoretical two- and three-dimensional flow models are used to investigate the effects of the spatial variability of the hydraulic conductivity on the underground flows. The role of the connectivity in generating flow channelling is examined thanks to the observation of close relations between the permeability and the hydraulic pressures. The sensitivity analysis shows clearly that the relation between local permeability and hydraulic pressures is not straight, and that the organization of the flows depends on the heterogeneity of the hydraulic properties and their spatial correlation. Strong channelling effects are observed in highly heterogeneous porous media. The development of flow channelling as a function of the variance of the natural log permeability values and the correlation lengths is demonstrated.

The integrated multi-disciplinary geological characterization at the *La Frasse* test site combined with the hydrogeological and lithological data of several additional case studies led to the proposal of a global conceptual model. The following assumptions are considered to enable a subsequent quantification of flow components:

- The flow occurs under confined to leaky conditions, with leakage varying in space;
- The flow framework is controlled by a complex multi-layer system, isolated lenses or perched aquifer;
- The aquifer system is divided into interconnected hydrological zones presenting various degrees of saturation;
- Each hydrological zone may function individually from the others;
- Horizontally and vertically, the flow direction in the porous matrix is affected by prevailing structural patterns generating channeling effects;
- The flow is multidirectional, free and channelized, and is affected by temporal and spatial changes;
- The aquifer is under an unsteady flow regime due to seasonal variation of natural gradients.

9.14

Simulation for a volcano monitoring network

Mautz Rainer*

* *Swiss Federal Institute of Technology (ETH), Institute of Geodesy and Photogrammetry, Wolfgang-Pauli-Str. 15, CH-8093 Zurich (mautz@geod.baug.ethz.ch)*

This paper investigates the capability of GNSS aided smart sensor network positioning based on Wireless Local Area Network (WLAN) signals incorporating access points, to monitor 3D deformation associated with volcanic activity and other comparable hazardous events. Many of the world's volcanoes that erupt, experience significant pre-eruption surface deformation. Internal magma pressure makes the surface bulge upwards and outwards. Thus, precise monitoring of surface deformation has the potential to contribute significantly to the realisation of a predictive capability of volcanic eruption. In particular, eruption source depth and evolution time can be estimated from surface deformation. The scale of this deformation is typically centimetric to decimetric over tens of square kilometres and over periods of weeks to years. Horizontal displacements show a radial pattern of movement of up to 10 cm with the displacement of the vertical components typically in the range of 4 to 6 cm per year.

In addition to the use of precise positioning information to facilitate deformation monitoring, the positioning function is vital for spatio-temporal referencing of the relevant multiple and complementary data types for volcano monitoring (e.g., seismicity, ground surface deformation, geothermal, gravity, and geomagnetic).

In architectural terms the monitoring network should consist of an array of distributed intelligent nodes (sensor motes), consisting of low-cost, commercially available, and off-the-shelf components (as far as possible) with built-in local memory and intelligence, with self-configuration, communication, interaction and cooperative networking capabilities. The nodes should be able to identify the type, intensity, and location of the parameters being measured, and collaborate in an inter-nodal manner with each other to perform distributed sensing for event confirmation and significance.

Because of the requirement for high accuracy positioning and the need to keep costs down (both in terms of technical complexity and power consumption), building carrier phase GNSS chips into all WLAN should be avoided. A compromise scenario is to have both types of nodes, some equipped with WLAN as well as carrier phase chips that are used for absolute coordinate referencing but with the majority of nodes with only WLAN communication and ranging capabilities. The limited GNSS aiding proposed should enable WLAN positioning to deliver centimetre level positioning. The sensors equipped with GNSS chips calculate their positions in a higher reference frame with high accuracy, and serve as anchor (= control or reference) points for the monitoring network. The communication function of the network should enable the exchange of the data required for positioning within the monitoring network. This should enable the WLAN nodes to position themselves exploiting inter-node distance measurements.

Such a monitoring system requires multiple key features including construction of the hardware that fulfil the requirements in terms of size, battery life and robustness, the extraction of ranges (distances) between sensor nodes, appropriate supporting network communications, protocol development, optimal routing and positioning. This paper addresses specifically the position function and characterises the performance of a novel high positioning algorithm using simulated range measurements. The 3D positioning algorithm uses the range observations for multilateration, clusterisation and geodetic network adjustment.

The novel algorithm is used to investigate various simulated positioning scenarios. The challenges associated with the use of wireless sensor networks are that ideally, the sensors (nodes) should have reliable positioning data, even in the presence of measurement noise, low inter-node connectivity and badly constrained geometry. This paper presents a strategy to enable

high integrity positioning and assesses its performance based on various parameters such as the node density, maximal signal range, required fraction of anchor nodes (which have GNSS positioning capability), range measurement errors, and locations of the nodes.

Presented are results from large simulated networks (i.e. 400 nodes) and the optimal network parameters are quantified. The requirement to have direct line of sights between stations can be solved by locating the nodes for a maximum number of directs sights. The number of required nodes depends on the transmission range. The required fraction of GNSS enabled reference nodes will be around 10%, depending on the network density.

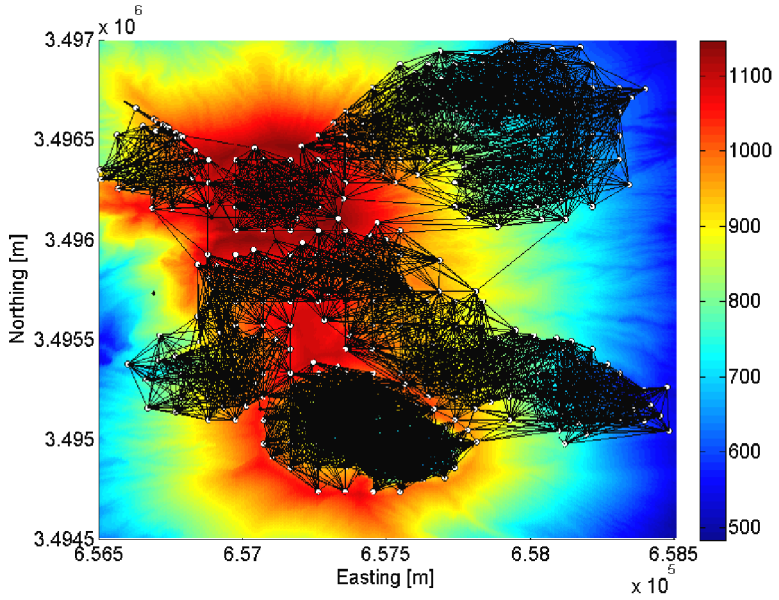

Figure 1. Optimised positions of 400 sensor nodes at volcano Sakurajima.

REFERENCES

Mautz, R., Ochieng, W.Y., Brodin, G. & Kemp, A. 2007:. 3D Wireless Network Localization from Inconsistent Distance Observations, Ad Hoc & Sensor Wireless Networks, Vol. 3, No. 2–3, pp. 141–170.

9.15

Systematic recording and analysis of natural hazards along railway lines using GIS

Andreas Meier, Christina Willi

SBB Infrastruktur, Umwelt; Naturrisiken; Schanzenstrasse 5, 3000 Bern 65

Due to the topographical conditions in Switzerland the SBB railway lines frequently are exposed to natural hazards as rockfall, debris flow, landslide, wind and others. The safe and high disposable train service is very sensitive to changes in the terrain. This asks for a high level of surveillance and preservation in the slopes along the railway lines.
Natural hazard data over the past 100 years and data about the currently prevailing risks exist in a variety of analogue and digital archives or databases. Therefore it is necessary to survey the data in time and space.
With the Geographical Information System for Natural Risks (GIS NR) consisting of the tools DERI NR and WebGIS the SBB established an important system for managing natural risks.

aging natural risks.

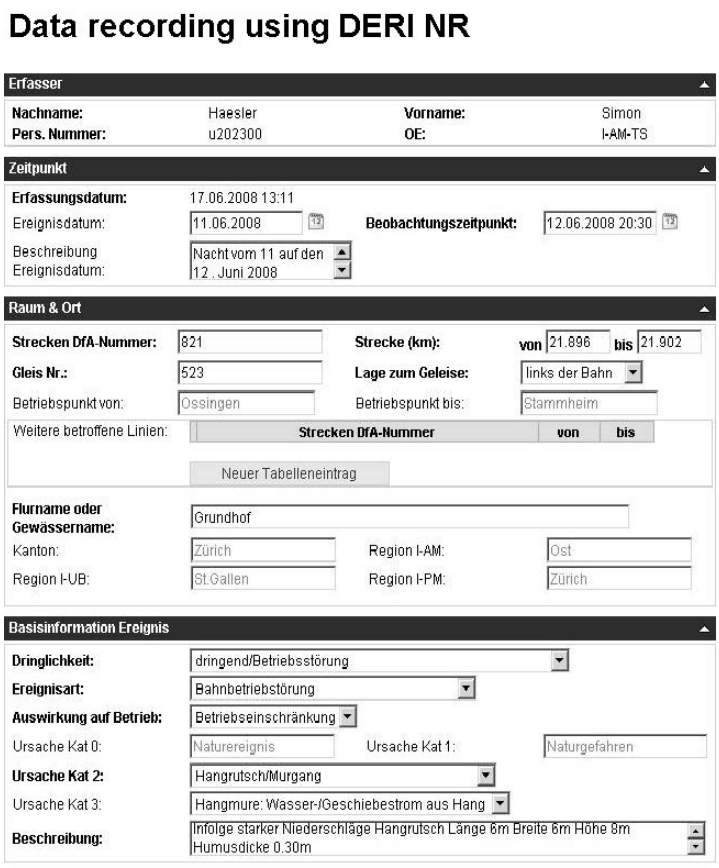

Figure 1. Graphical user interface of DERI NR

Data recording using DERI NR

DERI NR (Dérangements à l'Infrastructure „Natural Risks") is an instrument to report, record and document natural hazards. Events are continuously recorded in a central database (based on @enterprise technology; see figure 1) by the people in charge of maintaining safety.
In addition, during the next years historic data will be added. Thereby DERI NR becomes a constantly updated database of natural risks along the railway lines.

DERI NR is a workflow instrument with a two-step recording process. Train drivers, route inspectors and vegetation keepers register the key data of an event such as natural hazard type, route number and route position. The low number of obligatory data fields helps to report as many events as possible. Photographs and text documents can be attached.

Depending on the operating point and the type of hazard, the system forwards the report to the specialist for natural hazards. As a second step the event is fully documented. The recording ends with the evaluation weather more protection against natural hazards is needed. The recording process can be reactivated at any time, e.g. to add data from external risk calculations.

Visualisation in WebGIS

WebGIS is an application of Intergraph (BM3) and is open to all employees of SBB. It visualises the data from DERI NR on maps or orthophotos.
As a result of the second recording step the record appears in WebGIS. The user can select a specific area to overview previous hazards in the region. Natural hazards can be searched directly in WebGIS using DERI NR. Vice-versa, a double click on the visualised events opens the corresponding documentation in DERI NR.
The constantly updated risk map (figure 2) shows all sites that require more protection against natural hazards.

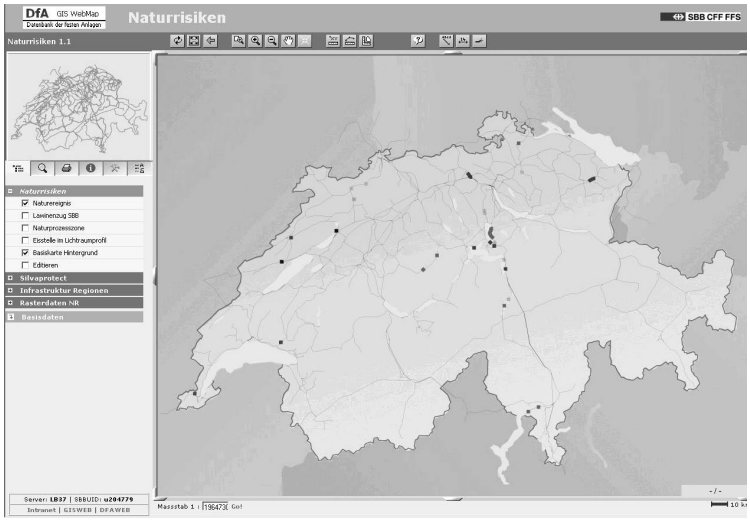

Figure 2. Map of current risk sites

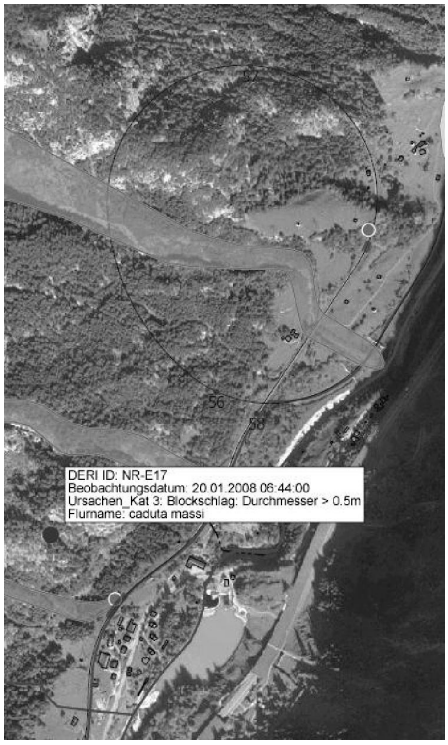

Figure 3. Natural hazards in WebGIS

Further extensions

Today GIS NR mainly centralises the documentation of natural hazards. Additionally the system offers queries about ice falls and avalanches at the Gotthard line and provides natural hazard maps from SILVAPROTECT.

In the coming years GIS NR will be a data base containing all information needed for the evaluation of risk sites.
Henceforth GIS NR provides the inventory and the condition of protective systems such as dams, warning systems, monitors, protection forests and others as well as calculated risk data, hazard maps and protection targets.
GIS NR helps inspectors and the technical management to decide about protection measures. In addition to the visualisation, tools for spatial data analysis will be available.

REFERENCES

Meier, A. 2008: Naturgefahren: Herausforderung für die SBB. Geomatik Schweiz, 5, 242-243.

9.16

Glass and magnetitic Spherules associated whit The bolid impact and mass extinction in D/C boundary in Central Alborz mountain north of Iran

Mahin Mohamadi

Geology Department, Payame Noor University, PNU.Iran .P.O.Box 19395-4697, Tehran, Iran. Mahin_mohamadi@pnu.ac.ir

Many glass spherules and tear like and also magnetitic and metallic spherules and dumb bell have income in upper part of Geirud Formation in central Alborz mountain. The grey marly limestone bed in upper part of geirud formation (upper Devonian) in Geirud valley, north of Tehran consist of many tear and spherule like yellow glass and also plentiful numbers of metallic and magnetitic spherules and dumb bells whith high density. Lower Carboniferous Mobarak Formation cover this bed in area.
All of these particles is collected and have been photographed by SEM. The form of These particles are similar, (but in different stratigraphic level) to those previously described from F/F boundary in many part of the world and from Kellewaser mass extinction, Claeys, P.,1994-1996, Sandberg,C. and all,1988 and McLaren,D.and all,1982. The biostratigraphy of this bed based on conodont is upper famennian (younger than expanasa zone). (mohammadi and all, in prep.) These spherules are likely to be produced by bolid impact event and may caused big mass extinction at that time which is marked by Hangenberge event .This is the first report of the presence of tektite and magnetitic spherules in D/C boundary layers of Iran and more inspection is needed from other equal layer from other part of country and also chemical and XRD analysis will be done as soon as possible for campaign whit the world samples.

REFRENCES :

Claeys,P.and all,1996 : Geochemistry of the Frasnian_ Famennian Boundary In Belgium : Mass extinction, anoxic ocean and microtektite layer, but not much iridium? Geological Society of America,Special paper 307 .pp,491-505

Claeys,P.and all,1994 :Microtektite-like impact glass associated whit the Frasnian-Famennian Boundary mass extinction, Earth and Planetary Science Lettres,V.22,Issues 3-4, pp,303-315

McLaren,D.and all,1982: Frasnian –Famennian extinction.in Silver,L., T., and Schultz,P.H., eds., Geological implication of Impacts of large asteroids and comets on the earth, Geological Society of America,Special paper 190,pp.477-483

Sandberg,C.A.and all,1988 : Late Frasnian mass extinction : Conodont event stratigraphy global changes and possible causes : Courier Forschungsinstitut Senkenberg, v.102, PP 267-307.

9.17
Geological and structural model of the Åknes rockslide (Norway)

Oppikofer Thierry*, Martina Böhme**, Lars Harald Blikra**, Marc-Henri Derron**, Michel Jaboyedoff*, Saintot Aline**

*Institute of Geomatics and Risk Analysis, University of Lausanne, Amphipôle, CH-1015 Lausanne (thierry.oppikofer@unil.ch)
**Geological Survey of Norway, Leif Eiriksons vei 39, NO-7040 Trondheim

Åknes is a complex rockslide situated on the flank of a famous fjord in Western Norway (Fig. 1a). The rockslide has a volume of >35 million m^3 (Derron et al., 2005) and is investigated and monitored within the Åknes/Tafjord Project, since its failure might cause a catastrophic tsunami in the fjord. A large series of geological, structural, geophysical and borehole investigations and several slope movement monitoring techniques make the Åknes rockslide one of the most intensively studied sites in the world (Ganerød et al., in press).

This study focuses on the conceptual model of the Åknes rockslide based on displacement measurements, digital elevation model analysis, terrestrial laser scanning, and field investigations. The understanding of the mechanism is crucial to implement suitable monitoring and early-warning systems.

Towards the SW and the NE, the rockslide body is delineated by two regional NNW-SSE faults (Fig. 1b). Sub-vertical NNE-SSW trending faults laterally delimit rockslide compartments and act as transfer surfaces. The main folds have a gently plunging ESE-trending axis crossing obliquely the landslide body. Vertical gneiss foliation (S1) near the hinge zones creates weaknesses and favourably orientated planes that lead to the formation of extension failures acting as back-cracks. Such a fracture led to the creation of a fast-moving ridge and a 30 m wide trench in the upper rockslide part and several rockslide scars on the slope are exactly located at the folds hinges with sub-vertical S1.

The observed displacements permit to divide the rockslide into several parts that move with different velocities and/or directions (Fig. 1c). Since most of the sliding surfaces reactivate S1, variations in the orientation of S1 – due to folds and undulations – create changes in the sliding direction between SE and SSW. The sliding surface is not continuous, but stepped by sub-vertical fractures perpendicular to the main sliding direction, that have been clearly identified on the topography in the vicinity of Åknes landslide (Oppikofer & Jaboyedoff, 2007). A model for this upper-most part of the rockslide implies a combination of planar sliding along S1, subsidence due to stepped failure surface and toppling towards the opened graben structure (Fig. 1d) (Oppikofer et al., 2008).

This interpretation gives a coherent framework of the movements obtained by various methods and leads to a reinterpretation of the morphology, indicating that several rockslides occurred in the past. These findings enable to establish the failure surface topography and to define blocks most susceptible to failure.

Figure 1. a) Picture of the Åknes rockslide (Derron et al. (2005)); b) Rockslide morphology displaying the back-scars, lateral transfer zones and the regional faults; c) Annual displacement vectors (data from Ganerød et al. (in press)); d) Instability model for the fast-moving ridge (from Oppikofer et al. (2008)).

REFERENCES

Derron, M.; Blikra, L. H. & Jaboyedoff, M. 2005: High resolution digital elevation model analysis for landslide hazard assessment (Åkerneset, Norway). In: Landslides and Avalanches: ICFL 2005 Norway, 101-106. Taylor & Francis Group, London.

Ganerød, G. V., Grøneng, G., Rønning, J. S., Dalsegg, E., Elvebakk, H., Tønnesen, J. F., Kveldsvik, V., Eiken, T., Blikra, L. H., & Braathen, A. in press: Geological Model of the Åknes Rockslide, western Norway. Eng. Geol.

Oppikofer, T., & Jaboyedoff, M. 2007: Åknes/Tafjord project: DEM analysis of the Rundefjellet/Tårnet area. Report, University of Lausanne, Switzerland, p.44.

Oppikofer, T., Jaboyedoff, M., Blikra, L. H., & Derron, M.-H. 2008: Characterization and monitoring of the Åknes landslide using terrestrial laser scanning. Proceedings of the 4th Canadian Conference on Geohazards, 211–218. Presse de l'Université Laval, Québec, Canada.

9.18

A new approach to dating carbonate-lithic rockslides

Ostermann Marc* & Sanders Diethard*,

*Geologisch-Paläontologisches Institut, Innrain 52, A-6020 Innsbruck
(marc.ostermann@uibk.ac.at)

Large-scale rockslides exceeding 106 m^3 in volume not only are a major process of mountain erosion and orogenic mass balance but, in densely populated regions such as the Alps, also represent a major threat to humans and facilities. Establishing the distribution of rockslides in time is a prerequisite of hazard assessment for future events and for a better understanding of potential triggers, such as climatic change or phases of enhanced earthquake frequency and post-glacial stress relaxation (e.g. Erismann & Abele, 2001).

In the last decades, rockslide deposits were dated by ^{14}C age determination of wood fragments that are preserved (a) in lacustrine or fluvial successions underneath the rockslide mass, (b) within the rockslide mass, or (c) in newly-formed lakes on top of the sturzstrom (e.g. Wassmer et al., 2004). In each case, the ^{14}C age provides a different constraint for the age of the rockslide event, that is, in case (a) the ^{14}C age represents a maximum age limit for the event, in case (b), which is very rare, the ^{14}C age is a good proxy age of the event, and in case (c) the ^{14}C age provides a minimum age limit. Unfortunately, the ^{14}C approach to age-dating often cannot be applied because of absence of suited deposits or exposures thereof, lack of organic remnants or of remnants suited for age-dating, and/or because the resulting ^{14}C age is fraught with marked imprecision (e. g. Prager et al., 2008).

In the past decade, an increasing number of sturzstroms have been dated by ^{36}Cl exposure dating of detachment scars and/or of surfaces of boulders within the sturzstrom deposit (Ivy-Ochs et al., 1998). At the present state, thus, an increasing number of the numerous Alpine rockslides that hitherto could not be determined by the ^{14}C method will foreseeably be dated by exposure dating, but a cross-check with another method of age determination is desirable in each case.

Our preliminary investigations of major carbonate-lithic rockslides of the Alps revealed that indeed nearly all of them contain pockets, thicker crusts and patches wherein the rockslide material underwent cementation into a breccia. These breccia cements can provide a proxy age of the sturzstrom event by dating the cement with the $^{234}U/^{230}Th$ disequilibrium method (Ostermann et al., 2007). To this end, careful petrographic analysis of samples is necessary to distinguish different generations and types of cement.

Within the research project: Catastrophic Rockslides in the Alps, funded by the Austrian Science Fund, age determination of 17 selected rockslides (Fig.1) shall be done by both U/Th dating of cements and by surface exposition dating with cosmogenic radionuclides. Yet exposition dating has the undisputed advantage that it is the only method that veers for the 'real' age of a sturzstrom event. Combining the precision of U/Th ages with the correctness of (often more blurred) exposition ages was, therefore, the ideal approach to determine most precise ages for selected Alpine landslides.

REFERENCES

Erismann, H. T. & Abele, G. 2001: Dynamics of Rockslides and Rockfalls. Springer, Berlin, Heidelberg, New York, 316pp.

Ivy-Ochs, S., Heuberger, H., Kubik, P.W., Kerschner, H., Bonani, G., Frank, M. & Schlüchter, C. 1998:The age of the Koefels event - relative, 14C and cosmogenic isotope dating of an early Holocene landslide in the Central alps (Tyrol, Austria), Zeitschrift f. Gletscherkunde u. Glazialgeologie 34, 57-70.

Prager, C., Ivy-Ochs, S., Ostermann, M., Synal, H.-A. & Patzelt, G. 2008: Geology and radiometric ^{14}C-, ^{36}Cl- and Th-/U-dating of the Fernpass rockslide (Tyrol, Austria). Geomorphology, in press.

Ostermann, M., Sanders, D., Prager, C. & Kramers, J. 2007: Aragonite and calcite cementation in 'boulder-controlled' meteoric environments on the Fern Pass rockslide (Austria): implications for radiometric age-dating of catastrophic mass movements. Facies 53, 189-208.

Wassmer, P., Schneider, J. L., Pollet, N. & Schmitter-Voirin, C. 2004: Effects of the internal structure of a rock-avalanche dam on the drainage mechanism of its impoundment, Flims Sturzstrom and Ilanz paleo-lake, Swiss Alps. Geomorphology 61, 3-17.

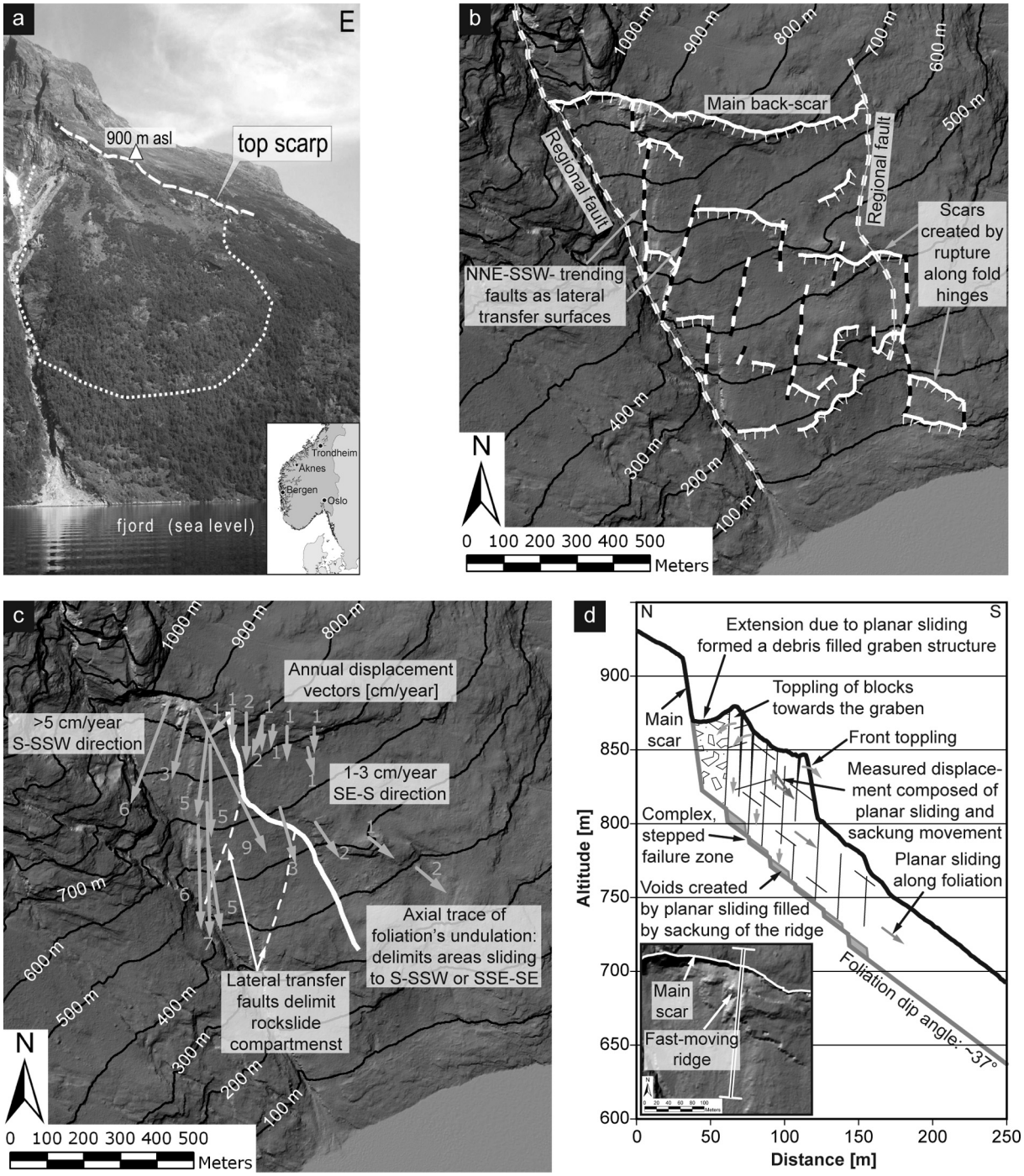

Figure 1. Overview map of the Eastern, Southern and most of the Western Alps with prominent carbonatelithic rockslide deposits. Rockslide deposits chosen for further investigation are highlighted by white framed pentagons.

9.19

The role of regional fault and fold-related fractures in the development of rock slope failure

Pedrazzini Andrea*, Jaboyedoff Michel*, Froese Corey **, Humair Florian *, Langenberg Willem**, & Francisco Moreno**

*Institute of Geomatics and Risk Analysis, University of Lausanne, Amphipôle (andrea.pedrazzini@unil.ch)
**Alberta Geological Survey, Edmonton, Alberta, Canada

Large rock slope failures in fracturated rock are often controlled by the combination of pre-existing tectonic fracture and brittle fracture propagation in the intact rock mass during pre−failure phase (Brideau et al, in press). Tectonic features such fold and large fault have in important influence on the frequency and the spatial distribution of large rock slope failure (Ambrosi and Crosta, 2006). In this paper, we focus on the influence of the tectonic features in the kinematic release but also on the control of the local reduction of rock mass proprieties induced by tectonic damage.

We present here the case study of Turtle Mountain, south-western Alberta, Canada. This area is characterized by the presence of the famous Frank slide, occurred in 1903 and involving 30 mio of m^3 of massif limestone. From a structural point of view the area is characterized be the presence of the Turtle Mountain anticline and the Turtle Mountain thrust. The Turtle Mountain fold could be described as a modified fault-propagation fold.
A detailed field mapping and the morpho-structural analysis (Jaboyedoff et al., in press) the high resolution digital elevation model (HRDEM) allows identifying at least 5 discontinuity sets. Based on the location their orientation three joint sets (J2, J3, and J4) could be related to the folding phase:

1) A persistent extensional joint, sub-parallel to the fold axis and mainly persistent in the hinge area.
2) Two strike-slip conjugate fractures manly persistent in the western fold limb.

The other two joint sets (J1 and J5) have with a dominant feature and cutting the entire Turtle Mountain anticline. The large persistence and their occurrence suggest that these discontinuities are post-folding and related to the NE-SW transpression during Eocene (Price et al., 1986).
In order to quantify the rock mass quality in the different portions of the Turtle Mountain anticline the Geological Strength Index (GSI) was estimated (Hoek and Brown, 1997). In the fold limbs the GSI value range between 35 to 55. the GSI decrease progressively in the hinge area and ranges between 20 to 35. The variation of the GSI values along the fold could by explain an increasing of fracturation (especially discontinuity sets J2) near the hinge zone due to the strain concentration during the folding phase. At the same time an increasing of fracturation in this area increase the susceptibility of the rock mass to weathering or freeze and thaw cycle.
Field mapping shows that hinge area correspond also the area were most of the past and potential instability are concentrated (Figure 1).
In this context two main potential failure mechanisms have been detected:

1) A planar sliding on bedding planes or persistent J1 discontinuity set with the rear release following extensional or the wedge formed by strike-slipe conjugate faults.
2) A toppling-sliding mechanism developed on the extensional fracture.

All this observations have been taking into account in order to asses the stability of the potential unstable areas in Turtle Mountain and to reexaminate the Frank slide mechanism.

REFERENCES

Brideau, M-A., Ming Y., Stead, D. (in press).The role of tectonic damage and brittle rock fracture in the development of large rock slope failure. Geomorphology (2008), doi:101016/j.geomorph.2008.04.010

Ambrosi C. and Crosta G.B. (2006): Large sackung along major tectonic features in the Central Italian Alps. Engineering Geology, 83 183-200.

Jaboyedoff, M., Couture, R. and Locat, P. (in press): Structural analysis of Turtle Mountain (Alberta) using digital elevation model: toward a progressive failure. Geomorphology. (2008). doi:10.1016/j.geomorph.2008.04.012

Price R.A. 1994. Geological history of the Peace River Arch [accessed June 2004]; In Geological Atlas of the Western Canada Sedimentary Basin, Mossop G.D., Shetson I. (comp.), Canadian Society of Petroleum Geologists and Alberta Research Council, Calgary, Alberta, URL http://www.ags.gov.ab.ca/publications/ATLAS_WWW/ATLAS.shtml.

Hoek, E., Brown, E.T., 1997. Practical estimates of rock mass strength. International Journal of Rock Mechanics and Mining Sciences 34, 1165−1186.

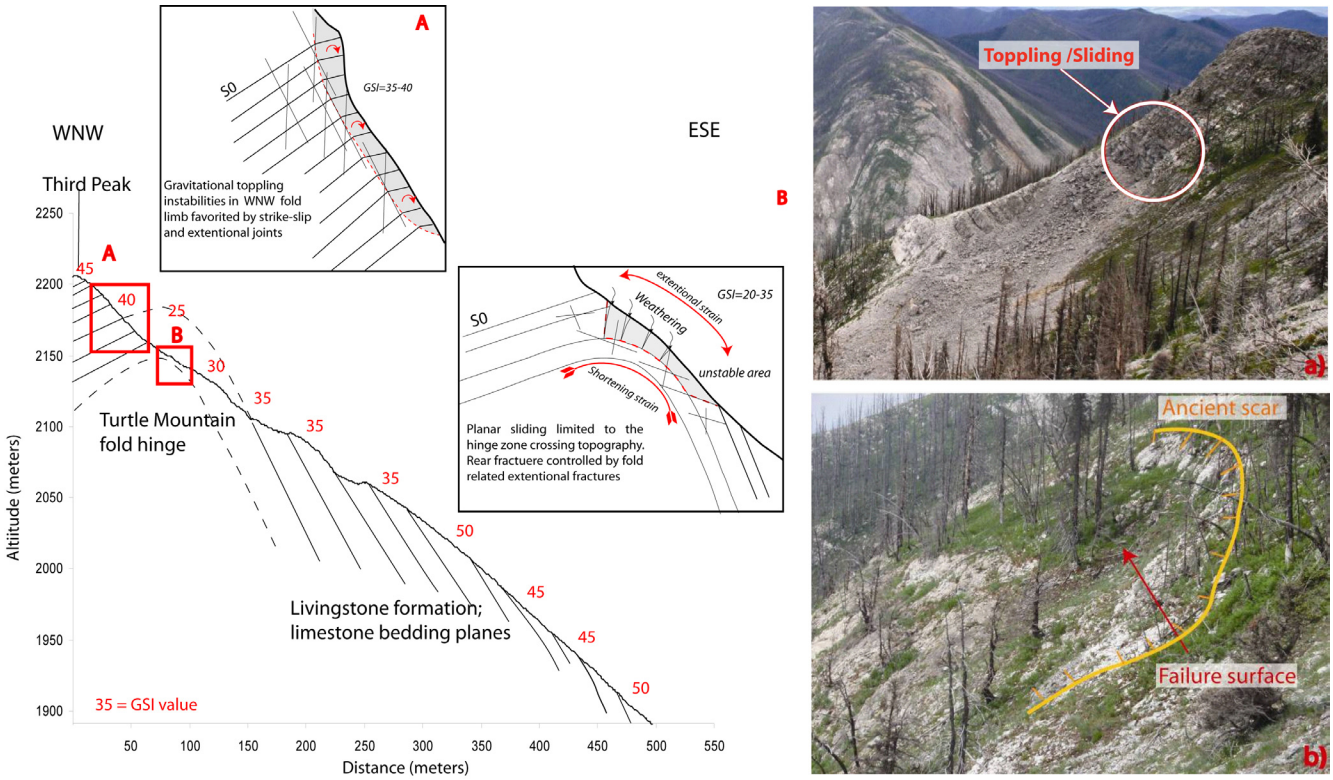

Figure 1: (left) Failure mechanisms driven by fold related fractures affecting the hinge zone of Turtle Mountain anticline. The numbers on the profile correspond to the evolution of the GSI value. (right) Pictures show field evidence of past instabilities related to the fold location.

9.20

The earthquake loss estimating tool QLARM: Applications in real-time and for predictions

Rosset Philippe*, Bonjour Cyrill**, Cua Georgia**, Kaestli Philipp**, Trendafiloski Goran*, Wiemer Stefan** & Wyss Max*

*World Agency for Planetary Monitoring and Earthquake Risk Reduction (WAPMERR), 2 rue de Jargonnant, CH-1207 Genève (p_rosset@wapmerr.org)
**Swiss Seismological Service, ETH Hönggerberg CH-8093 Zürich

QLARM is a loss-estimating tool being constructed jointly by WAPMERR and the Swiss Seismological Service. This computer program and its standard world dataset will be available for use by any professional. Its purpose is to calculate mean damage to the built environment and human losses in case of earthquakes anywhere in the world. The world data sets we are currently updating include: Population, building stock, attenuation of seismic waves, local soil conditions, critical facilities, and regional earthquake source properties.

The population is given by number of inhabitants down to the smallest settlements available for each country. QLARM is thus able to rank settlements according to the severity of losses, which is useful for rescue teams in earthquake disasters.

The building stock is distributed in vulnerability classes of the EMS-98 scale. This distribution is a function of the region and of the settlement size. The information on building quality comes from the World Housing Encyclopedia, from the literature, satellite images, ground surveys, and expert opinion.

Attenuation functions are taken from the literature and by calibration. Although it is clear that regional differences exist, they are not well quantified. In some areas we may need to modify the attenuation relationship such that intensities observed in past earthquakes are matched.

Soil properties are defined in varying detail for important cities worldwide in the literature. We derive amplification factors (for intensity or acceleration) as well as we can from published data on soil properties, microzonation maps, geological maps, and topography.

The most probable depth for shallow earthquakes is a parameter we are mapping by region because the need for this parameter arises in real-time loss estimates. We calculate losses for large earthquakes worldwide within less than an hour of their occurrence when there is only a teleseismic estimate of the depth available, with its large error. This poses a problem because losses depend crucially on the hypocentral depth.

An example of a loss estimate in real time is the Sichuan earthquake of the 12 May 2008. At first the magnitude was given as M7.5. Based on this, we distributed an email 28 minutes after the quake, giving 3,000 +/-1,000 as the most probable number of fatalities. As soon as information reached us that the magnitude may be M7.9, we revised our estimate to 40,000 to 100,000 fatalities (50 minutes after the event). Our alerts by email are distributed to anyone who requests them. Figure 1A shows the map of mean damage to settlements that we placed on our website for public viewing 52 minutes after the Sichuan earthquake (www.wapmerr.org).

Predictions of several earthquakes of class M8+ are currently in effect worldwide based on the MSc algorithm (Kossobokov, personal communication). We calculated losses that are expected to result in two of these cases, if the respective predictions should come true. The damage state resulting from a possible future large earthquake in central Chile is shown in Figure 1B. We expect that a major earthquake disaster is likely to occur in central Chile in the future with more than 1,000 fatalities.

To have some confidence in these results, we calibrated QLARM by verifying that the selected attenuation function and the building stock properties yield the intensities and human losses observed in past earthquakes in the region in question. Calibrating QLARM for different parts of the globe is an important ongoing activity. The parameters we consider modifying regionally include vulnerability curves, attenuation functions, distribution of buildings into classes, and the casualty matrix on which the number of fatalities and injured is derived for a given damage state.

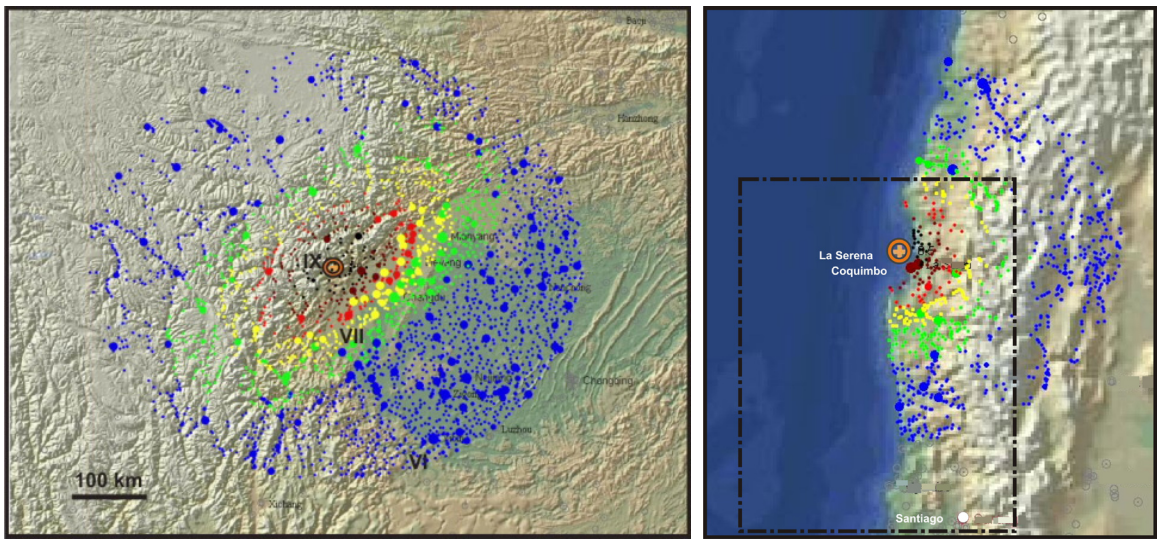

(A) (B)

Figure 1. Maps of mean damage state of buildings in settlements, (A) in the case of the Sichuan earthquake M7.9, May 12 2008, and (B) in a hypothetical scenario that may result in the future from a likely M8.5 earthquake off the coast of central Chile near a location for which a prediction is in effect.
The colour of the dots corresponds to the mean damage in settlements from black (major destruction) to blue (minor damage). The size of the dots is proportional to the population, the epicenter is marked by a ring and roman numerals indicate intensities.

9.21

On the predictability of snow avalanches

Schweizer Jürg

WSL Institute for Snow and Avalanche Research SLF, Flüelastrasse 11, CH-7260 Davos Dorf, email: schweizer@slf.ch

Snow avalanche are rare events and large avalanches that cause damage or harm to people can be called extreme events. In the general context of prediction and predictably of extreme events, we will examine whether snow avalanches are predictable based on a few examples of forecasts at different scales. Clearly, avalanche predictability depends on scale. When the regional avalanche danger is High or Very High, an avalanche is likely somewhere in the region. However, even at such high danger levels, the release probability in a single avalanche path is well below 50% (typically on the order of 1-10%). This means that a single avalanche is a rare event, which is not predictable even when higher danger levels prevail. At the lower danger levels – relevant for backcountry recreation – the release probability is significantly lower. The low release probability does not mean that the risk is low. Even with low occurrence probability the risk might be too high to be acceptable so that comprehensive preventive measures (e.g. temporary road closures) are required. Though the quality of snow avalanche forecasts is typically rather poor, i.e. the skill score in a statistical sense is low, low probability forecasts can be useful if large values are at stake.

9.22

A portable radar interferometer for the measurement of surface deformation

Strozzi Tazio, Werner Charles, Wiesmann Andreas & Wegmüller Urs

Gamma Remote Sensing, Worbstrasse 225, CH-3073 Gümligen ({strozzi,cw,wiesmann,wegmuller}@gamma-rs.ch; www.gamma-rs.ch)

Satellite radar interferometry has been used extensively for ground-motion monitoring with good success. In the case of landslides, glaciers and rock-glaciers, for example, space-borne radar interferometry has a good potential to get an overview on surface deformation. The role of space-borne radar interferometry as an element in a warning system is however constrained by the specific space-borne radar imaging geometry, the typical multiple-week repeat-interval, and uncertainties in the data availability. Most of these limitations can be overcome with an in-situ radar imaging system [1,2].

Gamma Remote Sensing has developed a portable radar interferometer that utilizes real-aperture antennas, each 2 meters in length, to obtain high azimuth resolution [3,4]. Images are acquired line by line while rotating the transmitting and receiving antennas about a vertical axis (Figure 1). The installation effort is relatively small and the instrument is portable and can be battery operated. Individual measurements can be taken in less than 15 minutes and the acquisition time is limited primarily by the speed of the rotational scanner. Each image line is acquired in approximately 2ms hence there is little or no movement of the scene to introduce temporal decorrelation.

Phase differences between successive images acquired from the same location are used to determine line-of-sight displacements δ from the differential phase ϕ via the relationship $\delta = -\lambda \cdot \phi / 4\pi$ where λ is the wavelength. The instrument operates at 17.2 GHz (Ku-Band, λ=17.4 mm) with a displacement measurement sensitivity better than 1 mm. The range resolution of the radar $\delta r = c/2^*B$ is determined by the 200 MHz bandwidth B and is equal to approximately 75 cm. Because this is a real-aperture imaging system, the azimuth resolution is determined by the antenna beamwidth and slant range R, $\delta az = R \sin \theta$. In the case of our terrestrial radar, the azimuth beamwidth is 0.4 degree yielding an azimuth resolution of about 7m at a slant range of 1km.

The instrument uses two receiving antennas with a short baseline to form an interferometer. Phase differences between simultaneous acquisitions by these antennas are used to calculate the precise look angle relative to the baseline, permitting derivation of the surface topography. Expected statistical noise in the height measurements is on the order of 1 meter.

In this contribution the design, measurement principles and characteristics of the portable radar interferometer are presented. Results obtained in a series of experiments started in September 2007 over glaciers (e.g. Rhonegletscher and Gornergletscher) and landslides (e.g. Tessina, Pian San Giacomo) are also discussed.

Figure 1. The portable radar interferometer deployed over the Gornergletscher showing the rotational scanner, antenna support structure, antennas, and microwave assembly.

REFERENCES

[1] Antonello G., N. Casagli, P. Farina, D. Leva, G. Nico, A. J. Sieber and D. Tarchi, Ground-based SAR interferometry for monitoring mass movements, Landslides, 1(1): 21-28, March 2004.

[2] Pieraccini M., L. Noferini, D. Mecatti, C. Atzeni, G. Teza, A. Galgaro and Nicola Zaltron, Integration of Radar Interferometry and Laser Scanning for Remote Monitoring of an Urban Site Built on a Sliding Slope, IEEE Trans. Geosci. Remote Sensing, 44(9): 2335-2342, 2006

[3] Wiesmann A., C. Werner, T. Strozzi and U. Wegmüller, Measuring deformation and topography with a portable radar interferometer, 13th FIG International Symposium on Deformation Measurements and Analysis and 4th IAG Symposium on Geodesy for Geotechnical and Structural Engineering, Lisbon, Portugal, May 12-15 2008.

[4] Werner C., A. Wiesmann, T. Strozzi and U. Wegmüller,Gamma's portable radar interferometer, 13th FIG International Symposium on Deformation Measurements and Analysis and 4th IAG Symposium on Geodesy for Geotechnical and Structural Engineering, Lisbon, Portugal, May 12-15 2008.

9.23

Rockfall modelling applied to rockfall protection design

Thüring Manfred

Istituto Scienze della Terra, Scuola Universitaria Professionale della Svizzera Italiana, CP 72, CH-6952 Canobbio (manfred.thuering@supsi.ch)

Rockfall modeling by computer simulations can be used to plan and design rockfall protection measures. RockSim3D is a recently developed software to simulate the three-dimensional process of rocks falling down a hill slope. The falling rocks are modeled as individual, dimensionless, spherical particles. The interaction with the digital representation of the terrain occurs at the center of the particles.

The computer program is a stand-alone Microsoft Windows application, reads and writes ESRI raster and shapefiles as input and output and needs a GIS (geographic information system) for pre- and post-processing of input and output. The software is developed in Microsoft Visual Studio and uses the open-source library GDAL for reading and writing GIS vector and raster files.

The main input of the software is a raster file which defines the digital terrain and the surface properties, and a shapefile

containing the starting locations of rock elements. A few models are available to simulate the impact phase of rock elements with the underlying terrain. The main outputs are shapefiles containing the three-dimensional rockfall trajectories and particle locations, attributed by information such as elapsed time, velocity, kinetic energy and elevation above terrain.
Recently the functionality to consider rockfall protection measures, such as fences and barriers was introduced in the software. The protective measures are read from a shapefile and are represented as two-dimensional structures in three dimensions. The protections have characteristics, such as height and maximum mechanical resistance against penetration.
During the down-slope movement of a rock element, impacts with the protective measures are searched for and recognized. Three cases can occur, when a rock element approaches a protection: (i) the protection is not high enough and the rock element jumps over the protection and continues its down slope trajectory (ii) an impact occurs between the rock element and the protection and the kinetic energy of the rock element is below the mechanical resistance of the protection, and the rock element is stopped, (iii) the kinetic energy of the rock element exceeds the resistance of the protection and the rock element penetrates the protection, continuing its downhill trajectory with a residual velocity. As a variant, low-angle impacts between rock elements and protections can lead to a reflection of the rock element.
For each protective measure important information, such as number of impacts, or maximum encountered impact energy is saved and can be used for later analysis.
The introduction of protection fences and barriers enables the modeler to place these elements on the digital terrain and assess their efficiency by conducting rockfall simulations. In an iterative process, both the rock elements (i. e. their starting position, number and mass), and the protective measures (position, extension, height and maximum mechanical resistance) can be varied to determine their optimal position and design.
A case study is presented where the software is used to optimize the design and position of rockfall protection fences.

9.24

Hazard and risk assessment of landslides on accumulation reservoirs – a field applicable scheme

Thüring Manfred*, Cannata Massimiliano*, Hammer Jürg**

*Istituto Scienze della Terra, Scuola Universitaria Professionale della Svizzera Italiana, CP 72, CH-6952 Canobbio (ist@supsi.ch)
**DRM Switzerland SA, CH-6952 Canobbio (hammerj@vt.edu)

Slope instabilities are a threat to accumulation reservoirs and corresponding down-stream areas due to possible slope collapse, generation of flood waves, dam overtopping and flooding of downstream areas. A simple and field-applicable assessment scheme, based on existing approaches, is presented to evaluate hazards and risks due to landslide collapse, in order to obtain a first and preliminary overview. The outcomes are used to support planning of further investigations.

The hazards that arise from the presence of landslides on the slopes of accumulation reservoirs are (Figure 1): (i) The slope instability damages the dam itself and buildings and infrastructure. (ii) The masses of a partial or complete slope collapse reach the reservoir lake and cause a pulse wave, which travels to and damages the dam and buildings and infrastructures. (iii) The pulse wave overtops the dam and causes flooding in the areas below the dam. These three hazard situations are discussed briefly and field-applicable assessment schemes are presented to preliminarily evaluate the hazards and estimate the connected risks in terms of worst case scenarios.

In a first step the primary hazard needs to be assessed, estimating the characteristics of the landslide mass and its path down slope. This is mainly done by field evidence. Key information needed is type of material of landslide, volume, elevation above lake level, inclination of trajectory and width of landslide. The maximum run-out of the hazard is estimated by the Fahrböschung-approach or is modeled, evaluating if the slope instability reaches the reservoir lake (Eisbacher & Clague 1984, Hungr 1995). With the previously obtained information the characteristics of the pulse wave which may be generated due to a slope collapse is estimated, using simple calculations (Huber 1997, Huber & Hager 1997). For this purpose a map view of the reservoir and a cross section of the dam is needed, where dam height and geometry, water depths, freeboard, and distances can be read from. From the calculations it is possible to estimate if dam overtopping occurs.

If the calculated wave is likely to overtop the dam, the consequences of dam collapse and flooding are estimated using methodologies that predict flood heights and velocities in downstream areas (Beffa 2000, BWG 2002). Data obtained from maps or by field inspections is needed, such as valley geometry, roughness and inclination. The vulnerability assessment of the flooded areas is done based on maps or field inspections, such as number and type of flooded objects. The assessment gives an estimate of values and fatalities at risk.

The scheme is field-applicable with data usually available or that can be produced on-site and delivers a preliminary assessment of hazards and risks connected to the presence of landslides on the slopes of accumulation reservoirs. We present and discuss the scheme and show its application in a project in Romania, where a preliminary screening on a number of reservoirs was conducted to identify key characteristics in terms of hazard and risk.

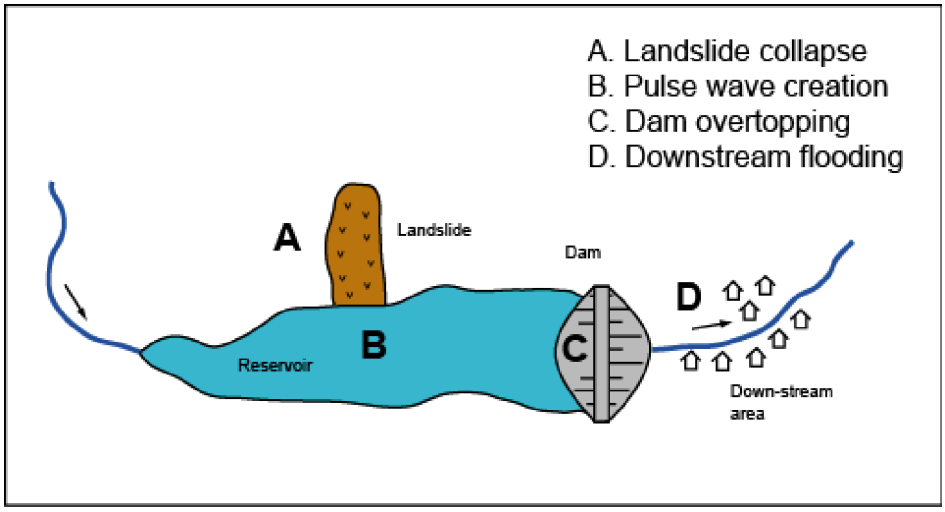

Figure 1. Hazard and risk situations due to the presence of a landslide on an accumulation reservoir.

REFERENCES

Beffa C. (2000): Ein Parameterverfahren zur Bestimmung der flächigen Ausbreitung von Breschenabflüssen, Wasser, Energie, Luft, No. 93, Heft 3/4.

BWG (2002): Sicherheit der Stauanlagen, Basisdokument zu den Unterstellungskriterien. Berichte des BWG, Serie Wasser.

Eisbacher G.H., Clague J.J. (1984): Destructive Mass Movements in High Mountains: Hazard and Management. Geological Survey of Canada, Paper 84-16.

Huber A. (1997): Quantifying impulse wave effects in reservoirs. 19 ICOLD Congress Florence Q.74(R.35), pp. 563-581.

Huber A., Hager W.H. (1997): Forecasting impulse waves in reservoirs. 19 ICOLD Congress Florence C(31), pp. 993-1005.

Hungr O. (1995): A model for the runout analysis of rapid flow slides, debris flows and avalanches. Canadian Geotechnical Journal, 32(4):610-623.

9.25

Landslide investigation by means of PSiNSARTM radar interferometry: the Piemonte experience

Carlo Troisi

ARPA Piemonte, Centro Regionale per le Ricerche Territoriali e Geologiche, via Pio VII 9, 10135 Torino, carlo.troisi@regione.piemonte.it , carlo.troisi@arpa.piemonte.it

PSiNSARTM technique (hereinafter PS technique) is a registered patent of Politecnico di Milano, Italy, and it is one of the Persistent Scatterers Methods, i.e. a group of applications which allow the use of satellite-born radar SAR (Synthetic Aperture Radar) interferometry to detect and measure ground deformations.

The PS Technique identifies single coherent benchmarks, referred to as Permanent Scatterers or PS, and reconstructs their displacement history. PS's are natural "radar targets" that are located across the earth's surface and can be monitored by satellites. When PS remain coherent within a multi-temporal radar data-set, it is possible to detect and measure millimeter variations in the sensor-target distance over time. PS's typically correspond to objects on man-made structures such as buildings, bridges, dams, water-pipelines, antennae, as well as to stable natural reflectors (typically bare exposed rocks faces). Starting with the identification of such PS's, the technique analyzes thousands of square kilometers of territory, within an extremely short time. Indeed, the PS's comprise a sort of "natural geodetic network" for accurately monitoring surface deformation phenomena, as well as the stability of individual structures.

Wherever PS's are present, it is possible to:

- Establish their geographic coordinates.
- Estimate their displacement rate along the Line of Sight (LOS) connecting the satellite and the radar ground target, with a precision which can be as good as 0.1 mm/a, depending on the amount of available data and the PS density.
- Reconstruct the displacement history of an individual PS where the precision can be as good as 1 mm on a single measurements.

All PS measurements can be easily downloaded onto Geographical Information Systems (GIS) and compared with other information layers, for better interpretation of results.
PS technique proved to be excellent for landslide investigation; since the maximum velocity which may be recorded by PS's is in the order of 10 cm/a, the technique is useful basically for slow-moving landslides. The main advantages are:

- Satellite radar images are available since 1992, so that it is possible to obtain displacement data since that year.
- A large number of slow-moving landslide can be cheaply identified and monitored over a wide area.
- There is no need for any field device, benchmark, monument etc., neither the monitored area needs to be accessible.
- Data are easily imported in GIS.

There are also, however, some problems:

- The method records only one component of the displacement, along the line-of-sight (LOS) between the satellite and the PS. The determination of total 3D displacements is not straightforward and may be troublesome.
- The method is not suitable to detect landslides with displacement rates exceeding about 10 cm/a along the LOS.
- The technique works as long as good radar reflectors are present (buildings, bare rocks etc.); in wooded or grass-covered areas it is not applicable. Moreover, unfavourable slope attitude, with respect to satellite acquisition geometries, leads to radar "shadowing" of wide areas. As a result, large portions of a given territory may be unsuited for PS technique. In the Piemonte experience (see below), about one third of the overall surface was totally blind to PS.
- Since satellite orbits are NS oriented, displacements along EW oriented slopes are difficult to detect.
- Since radar satellites pass over the same area once every 35 days (average), real-time landslide monitoring is not possible.
- PS analysis is no trivial matter. Few companies in the world provide this type of analysis
- If the target is affected by LOS displacement values approaching 14 mm between two successive acquisitions, measurements can be "aliased" and the estimation of the displacement may no longer be correct.

In the period 2005-2007 Arpa made a PS survey over the entire Piemonte, about 25000 km^2, the first case in the world of such a wide area surveyed with this technique. The survey was made using data from European radar satellites ERS 1 and 2, covering the time span 1992-2001. Since the main aim of the Arpa survey is landslide detection, this time span is extremely meaningful, for this period was affected by at least seven periods of very heavy or prolonged rains causing both floods and landslides. The survey identified about 2.2 millions PS, out of which about 10% show some displacement. To present the data for diffusion by a web-gis service on Arpa site (www.arpa.piemonte.it) we devised a method based on what we defined area anomala (anomalous area). An area anomala is defined as a polygon containing at least 3 PS's showing a displacement rate exceeding ± 2mm/a and likely to refer to a single definite phenomenon (landslide, subsidence, structural failure etc.). Up to now we defined about 2200 aree anomale. For each area it is possible to download a form describing all the relevant features.

The PS survey is proving extremely useful for the integration of the Piemonte landslide inventory, which includes, up to now, about 35000 landslides, mapped at the scale 1:10k (http://marcopolo.arpa.piemonte.it/website/geo_dissesto/arpa_ib_iffi/viewer.htm).

Up to now we mainly used PS's for:

- Identification and definition of formerly unknown landslides.
- Better definition of landslide limits.
- Definition of the state of activity.
- Zoning of large landslides.

Last, Arpa Piemonte is also experimenting the use of PS's for identification and definition of recent tectonic displacements. The first results are extremely promising.

9.26

Microzonage sismique du Canton de Fribourg: Carte de Sol de fondations

Vouillamoz Naomi* & Mosar Jon*

* *Département de Géosciences Université de Fribourg, Chemin du Musée 6, CH-1700 Fribourg (naomi.vouillamoz@unifr.ch)*

La coordination des cartes de sols de fondation à l'échelle 1 : 25'000 du canton de Fribourg vient terminer en juillet 2008 une étude de microzonage sismique lancée par l'Établissement cantonal d'assurance des bâtiments (ECAB) en collaboration avec la section Risques géologiques de l'Office fédéral de l'environnement (OFEV).
La norme SIA 261 défini 6 classes de sol de fondation (de A à F) sur la base des caractéristiques (lithologie, épaisseur et vitesse des ondes S) des 30 premiers mètres des couches superficielles. La cartographie des différentes classes de sols de fondation permet ainsi d'établir les données d'aléa sismique local. Ces données sont calculées à partir du potentiel d'amplification des ondes sismiques de chaque classe pour les 3 zones d'aléa sismique régional que comporte le canton de Fribourg (zones 1, 2 et 3a, approximativement du Nord au Sud). Cette démarche permet d'évaluer le risque sismique des agglomérations du canton d'une part et de définir le dimensionnement des bâtiments qui devrait s'en suivre d'autre part.
Les mandataires suivants ont participé à l'élaboration des cartes de sols de fondation pour les différentes parties du territoire cantonal fribourgeois délimitées par les feuilles de l'Atlas topographique suisse au 1 : 25'000 (Figure 1) :

- le bureau ABA-GEOL SA (Fribourg) pour les parts fribourgeoises des feuilles 1164 Neuchâtel, 1165 Morat, 1184 Payerne, 1204 Romont, 1244 Châtel-St.-Denis, 1245 Château-d'Oex, 1264 Montreux et 1265 Les Mosses ;
- le Département de Géosciences – Sciences de la Terre de l'Université de Fribourg pour les feuilles 1185 Fribourg, 1205 Rossens et 1224 Moudon ainsi que pour les klippes ou débordements non mandatés 1145 Bielersee, 1166 Bern, 1183 Granson, 1203 Yverdon-les-Bains et 1246 Zweisimmen ;
- le bureau Institut Géotechnique SA (Berne) pour les parts fribourgeoises des feuilles 1186 Schwarzenburg, 1206 Guggisberg et 1226 Boltigen ;
- le bureau Géoval Ingénieurs-Géologues SA (Sion) pour la feuille 1225 Gruyères.

L'élaboration des cartes se fait par l'interprétation en terme de classes de sols de fondation de différents types de données. Les cartes géologiques, les orthophotos, les modèles numériques de terrain (MNT 1m) et ombrages, servent d'information de base en ce qui concerne la nature du terrain. Les données de forages, la carte des instabilités et glissements de terrains du canton ainsi que des études géophysiques ponctuelles (géothermie, géoélectricité, géoradar, « petite sismique », ...) donnent des indications quand à la profondeur du substrat rocheux.
Les cartes de sols de fondation du canton de Fribourg ont été élaborées sous forme de SIG à l'aide de la suite de logiciels ArcGIS©. Une réactualisation continue est ainsi possible lorsque de nouvelles données sont à disposition. Lors de la synchronisation, une certaine systématique a été appliquée dans le but d'uniformiser les fichiers sources d'une part et de coordonner les bordures des cartes selon les mêmes critères d'autre part.

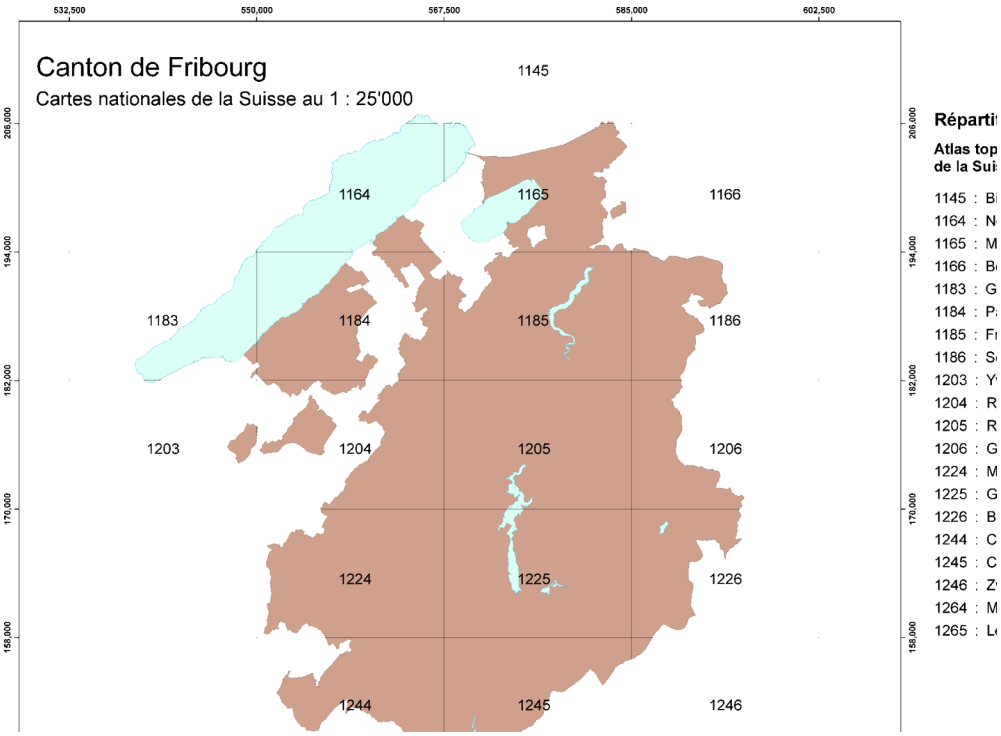

Figure 1. Carte de la répartition des feuilles 1 :25000 couvrant les canton fe Fribourg.

9.27

Effects of tectonic structures, groundwater pumping, and mining activity on evaporite subrosion and resulting land subsidence

Eric Zechner*, Ina Lewin**, Markus Konz*

*Geologisch-Paläontologisches Institut, Universität Basel, Bernoullistrasse 32, CH-4056 Basel (eric.zechner@unibas.ch)
** now at Institut für Angewandte Geowissenschaften, Technische Universität Darmstadt, Schnittspahnstr. 9, D-64287 Darmstadt (change of name from Spottke to Lewin 4/2008)

Evaporites of gypsum or rock salt are widely seen as the most soluble common rock formation. Percolating undersaturated groundwater leads to subsurface dissolution, or subrosion of evaporites and, consequently, to the development of karst. Depending on the hydrogeological setting and the anthropogenic circumstances, the subrosion may cause widespread land subsidence. Even comparably small subsidence rates can significantly affect sensitive urban infrastructure, such as larger buildings, dams, power plants, or the railway tracks for high-speed trains which cross the presented Muttenz-Pratteln site in Northwestern Switzerland.

For the observed widespread land subsidences several causes were considered: (1) natural dissolution of the evaporites of the Middle Muschelkalk (anhydrite and halite), which is induced by the tectonic setting with a set of Horst and Graben structures, (2) salt solution mining, which has been pursued at different locations over the last 150 years, (3) large-scale extraction of groundwater in the Upper Muschelkalk aquifer with successive hydrostatic connection along the normal faults. The tectonic setting of the study area is characterized by horst and graben structures delimited by normal faults. The construction of a 3D geological model included 47 faults and 4 faulted horizons of the main aquifers-aquitards boundaries and provided a basis for numerical groundwater modeling and the comparison with geodetic survey data (Spottke et al. 2005). The 3D numerical groundwater model was used to delineate areas with increased hydrostatic gradients. Intermediate scale laboratory experiments were conducted to understand density-coupled flow mechanisms in porous media. The setup of the density flow experiment was chosen to simulate the geological conditions found at the site (Konz et al. 2008). Recent land subsidences have been surveyed at 6 separate locations within the Muttenz-Pratteln area East of Basel, Switzerland. The diameters of the affected surface areas range from 100 to 1500 m, and corresponding subsidence rates reach more than 100 mm/year. Three sites show elongated shapes of depression cones along a SSW-NNE-oriented axis corresponding to the striking of the Horst and Graben structures, and, therefore, indicating a strong relation to the tectonic setting. The subsidence hazard area above each former or recent solution mining well was estimated based on a model concept, where the collapsed roof of excavated salt propagates with a 45 degrees angle to the surface. For three sites, which are salt solution mining fields, the predicted hazard area corresponds to the observed area of subsidence. One site, where solution mining has stopped more than 100 years ago, shows evidence that the initial cause for subsidence, i.e. solution mining, has been replaced by large-scale groundwater withdrawal initiating a significant hydrostatic gradient, which propagates along the graben normal fault network from the Upper Muschelkalk Aquifer to the evaporites of the Middle Muschelkalk. For the two last sites, a combination of a natural dissolution process due to the tectonic setting and a slightly increased hydrostatic gradient seems the most probable cause for the ongoing land subsidence.

REFERENCES

Konz, M., Ackerer, P., Younes, A., Gechter, D., Zechner, E. & Huggenberger, P. 2008: New homogeneous and heterogeneous laboratory-scale 2-D benchmark experiment for density-coupled flow models. Accepted to Water Resour. Res.

Spottke, I., Zechner, E. & Huggenberger, P. 2005: The southeast border of the Upper Rhine graben: A 3D structural model of geology and its importance for groundwater flow. Int. Jour. Earth Sci., 94, 580–593.